PB87-171187

Technical Discussion Related to the Choice of Photolytic Rates for Carbon Bond Mechanisms in OZIPM4/EKMA

North Carolina Univ. at Chapel Hill

Prepared for

Environmental Protection Agency
Research Triangle Park, NC

Feb 87

U.S. Department of Commerce
National Technical Information Service
NTIS

TECHNICAL REPORT DATA
(Please read Instructions on the reverse before completing)

1. REPORT NO.	2	3. RECIPIENT'S ACCESSION NO.
EPA-450/4-87-003		PB87-171187/AS

4. TITLE AND SUBTITLE	5. REPORT DATE
Technical Discussion Related To The Choice Of Photolytic Rates For Carbon Bond Mechanisms In OZIPM4/EKMA	February 1987
	6. PERFORMING ORGANIZATION CODE
7. AUTHOR(S)	8. PERFORMING ORGANIZATION REPORT NO.
H. E. Jeffries and Kenneth G. Sexton	
9. PERFORMING ORGANIZATION NAME AND ADDRESS	10. PROGRAM ELEMENT NO.
Dept. Of Environmental Sciences And Engineering University Of North Carolina Chapel Hill, NC	11. CONTRACT/GRANT NO.
12. SPONSORING AGENCY NAME AND ADDRESS	13. TYPE OF REPORT AND PERIOD COVERED
Air Management Technology Branch (MD 14) Monitoring And Data Analysis Division Office Of Air Quality Planning And Standards U. S. Environmental Protection Agency	14. SPONSORING AGENCY CODE

15. SUPPLEMENTARY NOTES

EPA Project Officer: Edwin L. Meyer, Jr.

16. ABSTRACT

This report proposes to explain the methods, and to identify the sources of information used to calculate photolytic rates, for the chemical models Carbon Bond III (CB3) and Carbon Bond IV (CB4) for use in the OZIPM3 and OZIPM4 oxidant modeling programs. The mixed layer photolytic rates described in Chapter 4 are also the default rates for CB4 in the OZIPM4 program, expected to be used in new State Implementation Plan calculations.

This report also reviews previous recommendations for photolytic rates used in the original OZIPP program and in the revised program OZIPM2.

17. KEY WORDS AND DOCUMENT ANALYSIS

a. DESCRIPTORS	b. IDENTIFIERS/OPEN ENDED TERMS	c. COSATI Field/Group
Photolytic Rates Chemical Bond Photochemical Model OZIPM Carbon Bond Model Oxidant Model State Implementation Plan		

18. DISTRIBUTION STATEMENT	19. SECURITY CLASS *(This Report)*	21. NO. OF PAGES
		70
	20. SECURITY CLASS *(This page)*	22. PRICE

EPA Form 2220-1 (Rev. 4-77) PREVIOUS EDITION IS OBSOLETE

United States
Environmental Protection
Agency

Office of Air Quality
Planning and Standards
Research Triangle Park NC 27711

EPA-450/4-87-003
February 1987

Air

PB87-171187

EPA

Technical Discussion Related To The Choice Of Photolytic Rates For Carbon Bond Mechanisms In OZIPM4/EKMA

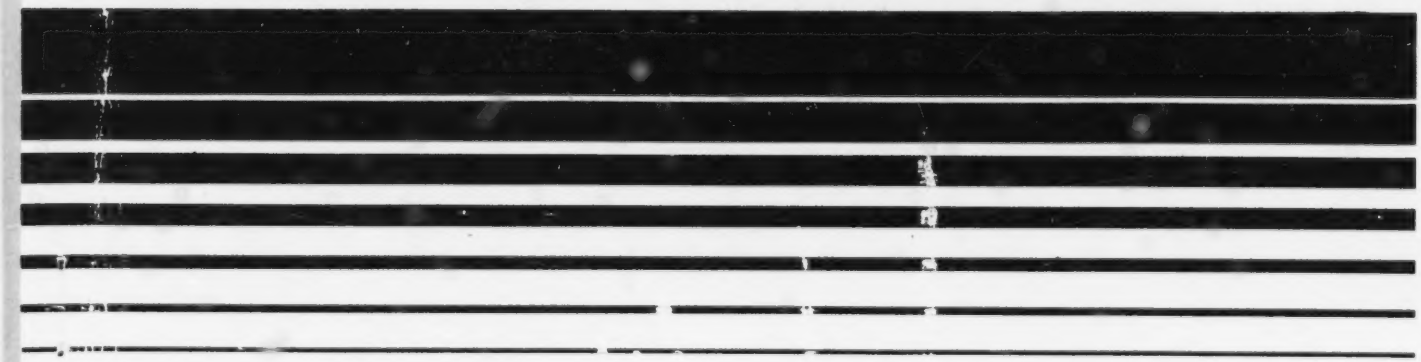

REPRODUCED BY
U.S. DEPARTMENT OF COMMERCE
NATIONAL TECHNICAL
INFORMATION SERVICE
SPRINGFIELD, VA 22161

Technical Discussion Related to the Choice of Photolytic Rates for Carbon Bond Mechanisms in OZIPM4/EKMA

H.E. Jeffries
Kenneth G. Sexton

Department of Environmental
Sciences and Engineering
University of North Carolina
Chapel Hill, NC 27514

Prepared For

Monitoring and Data Analysis Division
Office of Air Quality Planning and Standards

U.S. Environmental Protection Agency
Office of Air and Radiation
Office of Air Quality Planning and Standards
Research Triangle Park, NC

This report has been reviewed by the Office of Air Quality Planning and Standards, U.S. Environmental Protection Agency and approved for publication as received from the Principle Investigator. Approval does not signify that the contents necessarily reflect the views and policies of the Agency, neither does mention of trade names or commercial products constitute endorsement or recommendation for use.

Contents

1 Introduction 1

Purpose 1

The Photolysis Process 1

Photon Flux or Radiant Energy Flux 2
Radiation Models 9
Kinetics Parameters 10

Example Calculation 12

OZIPM Methods 12

Spectral Distribution of Rates 15

2 Review of Calculated Rates 18

Effects of Changes in Cross Section and Quantum Yield 18

Values Calculated For Carbon Bond III in OZIPM2 25

Nitrogen Dioxide Photolysis in CB3/OZIPM2 29
Carbonyl Photolysis in CB3/OZIPM2 29
Ozone Photolysis in CB3/OZIPM2 31
How CB3/OZIPM2 Rates Influenced CB4/OZIPM3/4 Rates 32

Affect of Altitude on Photolysis Rates 32

3 Atmospheric Rates 34

Measurements of Nitrogen Dioxide Photolysis Rates 34

Comparison of Theory and Measurement for Irradiance 34

UV Albedo 36

Adjustment of Calculated Actinic Flux for Albedo 41

4 Recommended Rates 45

Rates for Carbon Bond IV in OZIPM3/4 45
Surface Rates 45
Mixed Layer Rates 45
Recommended CB4 Photolytic Rates 46

Rates for Carbon Bond III in OZIPM3 46

Example Predictions Using New Rates 47
Simulation Conditions 48
Simulation Results 49

Figures

1. Extraterrestrial and Surface Solar Spectrum 4
2. Schematic Illustration of Gas and Aerosol Light Scattering Processes. 5
3. Example of Spectral Irradiance Components. 7
4. Sun's Position in Central NC For Five Months 8
5. Actinic or Spherical Irradiance 11
6. Calculation of Nitrogen Dioxide Photolysis Rate for Zenith Angle = 0°. 14
7. Relative Spectral Photolysis Rates 16
8. Photolysis Rates Calculated From Peterson 1976 Actinic Flux 27
9. Quantum Yields For Nitrogen Dioxide Photolysis 28
10. Examples of Measured Atmospheric Rates of Nitrogen Dioxide Photolysis. 35
11. Comparison of Radiation Model Predictions With Spectroradiometer Measurements. 37
12. Comparison of Horisontal and Spherical Irradiance. 38
13. Comparisons of Theory with Measurements for Atmospheric NO_2 Actinometry 44
14. Example Simulation Using CB4: Comparison of Surface and Mixed Layer Photolytic Rates 52
15. Example Simulation Using CB3: Comparison of Mixed Layer and 1984 Photolytic Rates 53
16. Comparison of CB3 and CB4 Using Mixed Layer Photolytic Rates 54
17. Comparison of CARB (CB3) and HCHO (CB4) Using Mixed Layer Photolytic Rates 55
18. Example Simulation Using CB4: 40% HC Control Using Mixed Layer Photolytic Rates 57
19. Example Simulation Using CB3: 40% HC Control Using 1984 Photolytic Rates 58
20. Comparison of Ozone-Hydrocarbon Relationships for CB3 and CB4 59

Tables

1. Calculation of Nitrogen Dioxide Photolysis Rate for Zenith Angle = 0°. 13
2. Definitions of Headings used in Photolytic Rate Tables 19
3. Theoretical Rates Used in EPA Models 20
4. Cross Sections and Quantum Yields Used. 26
5. Nitrogen Dioxide Photolysis Rate as a Function of Altitude. 33
6. Albedo Values Assumed by Peterson. 40
7. Albedo Values Measured by Dickerson, et al. 40
8. UV Albedo Values Measured by Doda and Green 41
9. Comparison of Higher Albedo Calculated Photolysis Rates with Atmospheric Measurements. 43
10. Recommended CB4 Surface Photolytic Rates 47
11. Altitude Adjustments Corrected For Albedo 47
12. Recommended CB4 Mixed Layer Photolytic Rates 48
13. Recommended CB3 Surface Photolytic Rates 49
14. Recommended CB3 Mixed Layer Photolytic Rates 49
15. Initial Conditions and Emissions Fractions 50

1

Introduction

Purpose

The purpose of this report is to explain the methods and identify the sources of information used to calculate photolytic rates for the System Applications, Inc. (SAI) chemical models Carbon Bond III (CB3) and Carbon Bond IV (CB4) for use in SAI's OZIPM3 and OZIPM4 oxidant modeling programs.[1] Both OZIPM3 and OZIPM4 programs are very similar; the former allows larger mechanisms to be used and has the Carbon Bond X mechanism built-in, while OZIPM4 is smaller and has CB4 as the default mechanism. The mixed layer photolytic rates described in Chapter 4 are also the default photolysis rates for CB4 in the OZIPM4 program. OZIPM4 is expected to be used in new State Implementation Plan calculations.

This report will also review previous recommendations for photolytic rates that were used in the original program, OZIPP[2], and in the revised program, OZIPM2.[3] In the last nine years these rates have undergone significant change. In addition, new measurements and analysis of irradiances in the UNC outdoor chamber suggest some major changes may be needed in the photolytic rates of the SAI developed models when these models are used in atmospheric simulations.

The Photolysis Process

Three factors determine the photolysis rate of a chemical species, S, in the atmosphere.

The first factor is the number of photons of a given wavelength (energy) moving through an area of space as a function of time, that is, the photons-cm^{-2}-sec^{-1}-nm^{-1}. This is often called the actinic flux and will be designated here by the script letter $\mathcal{A}_\lambda$. Actinic flux is a function of wavelength, λ, the solar zenith angle, χ, the altitude above the earth's surface, y, and the ground reflectivity or albedo, A.

The second factor is the ability of the species molecule to absorb photons, that is, the species absorption cross section (cm^2-molecule^{-1}) in the wavelength interval, designated here as $\sigma_\lambda(S)$.

The third factor is the fate of the molecule after it has absorbed a photon. That is, the number of species molecules that follow a particular reaction path after absorbing a photon, divided by the number of species molecules that absorbed photons in the wavelength interval. This fraction is called the quantum yield (a dimensionless number between 0 and 1) for a given process, and is designated here as $\Phi_\lambda(S)$.

The photolysis rate of species S at a given zenith angle χ, at an altitude y, and at an albedo A, will be designated as $J(\chi, y, A; S)$, and is calculated by:

$$J(\chi, y, A; S) = \int_{\lambda_1}^{\lambda_2} A_\lambda(\chi, y, A)\, \sigma_\lambda(S)\, \Phi_\lambda(S)\, d\lambda \qquad (1)$$

that is, the photolysis rate is the area under the product curve of photon flux, absorption cross section, and quantum yield as a function of wavelength. This area has units of time^{-1}. The radiant energy, or photon flux, A_λ, is common to all species; the kinetics parameters, σ_λ and Φ_λ, are unique for each species.

The lowest wavelength at which a species will photolyze (λ_1) is often determined by the lower limit of photon flux reaching the earth's surface (290–300 nm), while the highest wavelength (λ_2) is often determined by the cross section or quantum yield approaching zero at that wavelength.

Photon Flux or Radiant Energy Flux

Radiometric Quantities and Units

Radiant energy, Q_λ, is normally measured in joules. The relationship between wavelength, λ, and energy is given by Planck's law. The energy of a single photon is given by

$$Q_\lambda = \frac{hc}{\lambda}$$

where h is Planck's constant. Because 1 watt = 1 joule/sec,

$$h = 6.626176 \times 10^{-34} \quad \text{joule-sec}$$
$$= 6.626176 \times 10^{-34} \quad \text{watt-sec}^2$$

The speed of light, c, is

$$c = 2.99792458 \times 10^{8} \quad \text{meters-sec}^{-1}$$
$$= 2.99792458 \times 10^{17} \quad \text{nm-sec}^{-1}$$

Thus the energy of a single photon of wavelength λ is given by,

$$\begin{aligned} Q_\lambda &= 1.9864775 \times 10^{-16}\left(\frac{1}{\lambda}\right) \quad \frac{\text{joule-sec nm-sec}^{-1}}{\text{photon}}(\text{nm}^{-1}) \\ &= 1.9864775 \times 10^{-16}\left(\frac{1}{\lambda}\right) \quad \text{joule-photon}^{-1} \end{aligned}$$

Broadband, or spectrally integrated radiant energy is

$$Q = \int_{\lambda_1}^{\lambda_2} Q_\lambda \, d\lambda.$$

and is measured in joules.

Spectral radiant flux is dQ_λ/dt and is measured in watts-nm^{-1}. Broadband radiant flux, or just radiant flux, would be measured in watts.

Spectral radiant flux density, $\mathcal{E}_\lambda$, is radiant flux per area (a) or

$$\mathcal{E}_\lambda = \frac{dQ_\lambda}{da\,dt}$$

and the units are usually watts-m^{-2}-nm^{-1} or photons-cm^{-2}-sec^{-1}-nm^{-1}.

Radiant flux density incident on a surface is called *irradiance*.

Components of Radiation at the Surface

The radiant flux density outside the earth's atmosphere is called the extraterrestrial solar irradiance (H_λ). One of the most recent estimates of H_λ was produced by the World Radiation Center, Davos, Switzerland and was reported in Iqbal.[4] This spectrum is shown as the top line of Figure 1.

On their way to the earth's surface, many of the photons incident on the atmosphere undergo multiple scattering and absorption processes (see Figure 2). This not only partially depletes the radiant energy before it reaches the surface, it also affects the directional distribution of the photons. Notice that in Figure 2, the shape of the scattering intensity around aerosol particles is different from that around gas particles. This shape is a complex function of the aerosol optical properties. The component of the surface flux that is not scattered or absorbed is called the **direct normal spectral irradiance** (that is, the amount of energy, or photons of a given wavelength, per unit time incident on a unit surface that is perpendicular to the direct solar beam and coming only from $\approx 5°$ view of sky containing the sun).

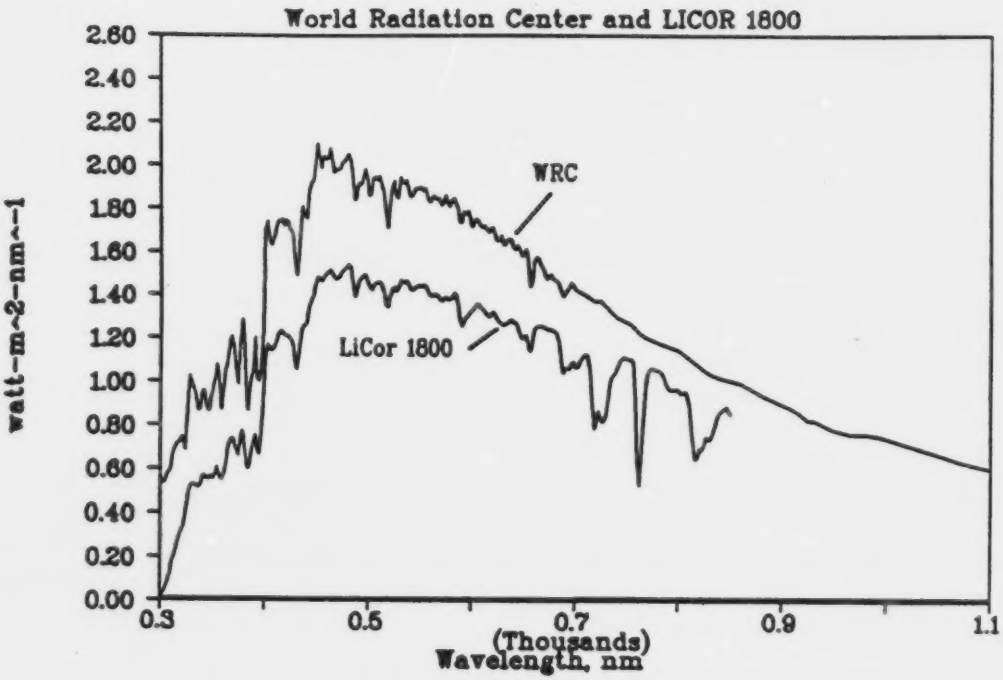

Figure 1. Extraterrestrial and Surface Solar Spectral Irradiance. Top: World Radiation Center recommended extraterrestrial solar irradiance, 2-nm resolution 300–700 nm, 10–20 nm resolution 700–1100 nm; Bottom: Measured surface global irradiance with LiCor 1800 spectroradiometer using 2-nm intervals and 4-nm resolution.

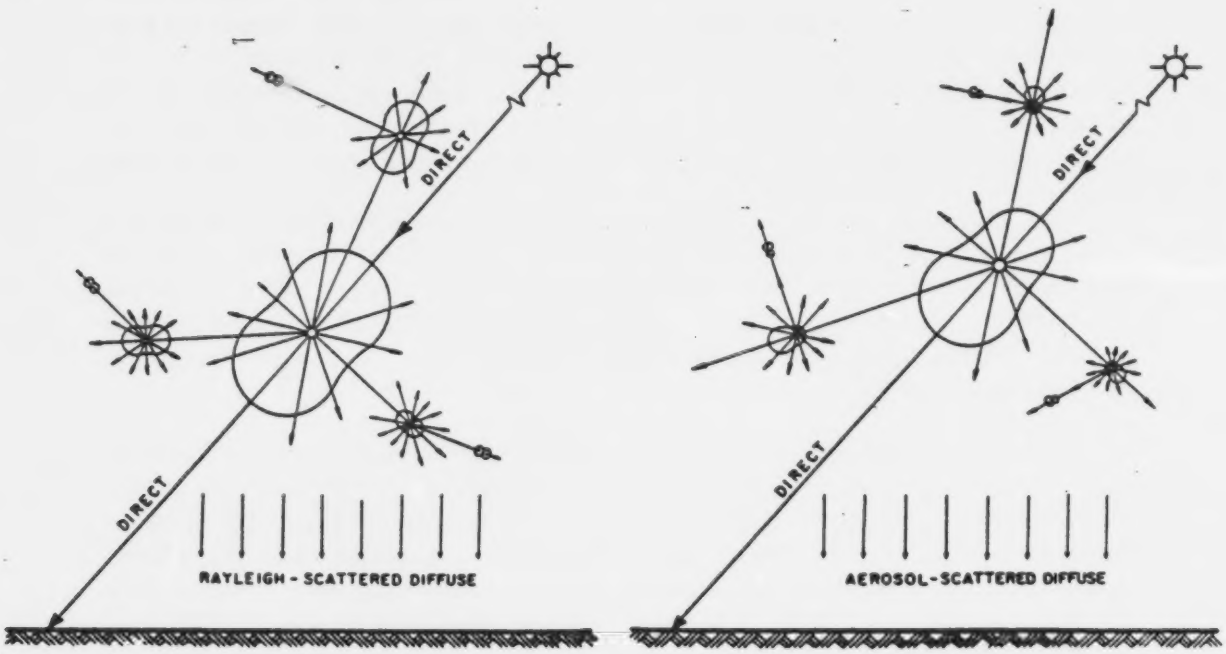

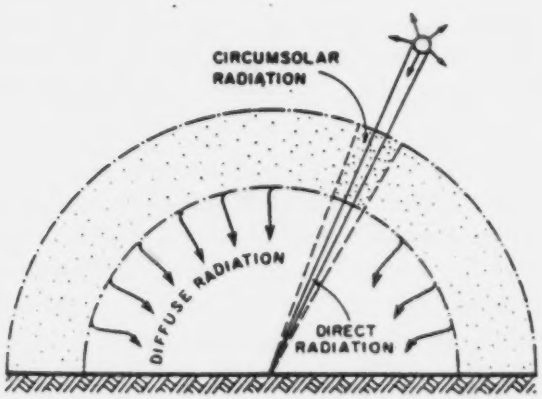

Figure 2. Schematic Illustration of Gas and Aerosol Light Scattering Processes (top). Bottom: Resulting direct and diffuse solar radiation components. (From Iqbal.[4])

Because many of the photons that are scattered from the direct beam undergo multiple scattering from gas molecules and aerosol particles, the component that is scattered can arrive at the surface from a full hemisphere (2π steradians). This sky light is called the **diffuse spectral spherical irradiance** (that is, the amount of energy per unit time incident on a unit sphere with no view restrictions). The diffuse spherical irradiance is often divided into downward and upward components.

The combination of direct normal and diffuse spectral spherical irradiance is called **global spectral spherical irradiance** ($\mathcal{G}_\lambda$). When the units of $\mathcal{G}_\lambda$ are photons-cm^{-2}-sec^{-1}-nm^{-1}, then the term "actinic flux" is often used. Some researchers have also used "actinic irradiance," "scaler irradiance," or "spherical irradiance." Without these qualifiers, the term irradiance generally means radiant flux on a horizontal, or flat, surface.

The spectral irradiance measured on a cosine response instrument, a so called "flat" receiver, at solar noon in central North Carolina on a clear day is shown as the bottom line in Figure 1. Figure 3 shows, in the ultraviolet range (300–400 nm), an example of the various spectral spherical irradiance quantities described above. Notice that, at wavelengths less than 370 nm, the diffuse component is larger than the direct component. This is because Rayleigh scattering is a strong function ($\approx \lambda^{-4}$) of wavelength.

As shown in Figures 2 and 3, not all of the radiant flux is downward. Part of the diffuse spherical irradiance is caused by the reflection of some of the incident radiation from surfaces, When the source of the incident radiation is the sun, the term "albedo" is commonly used instead of reflectance. In the meteorological literature, reflectance of the earth's atmosphere, as by clouds and air, is also called albedo.[4] In very general simple terms, the albedo (A) may be defined thus:

$$A = \frac{\text{Radiation reflected from a surface}}{\text{Radiation incident on a surface}}$$

This definition includes the surfaces of aerosols and gas molecules so that, for example, if one looks down from a location well above the ground, most of the reflected radiation is actually from the gas and aerosol below the viewpoint and only partly from the generally low reflection from the ground below. Of course, the reflected radiation is itself reflected, and thus multiple scattering produces additional flux in all directions. Albedo is usually wavelength dependent (spectral albedo, A_λ), and the integral, over wavelength, of the flux-weighted spectral albedo is called the integral albedo or just albedo (shown here without λ subscript), that is,

$$A = \frac{\int_{\lambda_1}^{\lambda_2} A_\lambda \mathcal{A}_\lambda \, d\lambda}{\int_{\lambda_1}^{\lambda_2} \mathcal{A}_\lambda \, d\lambda}$$

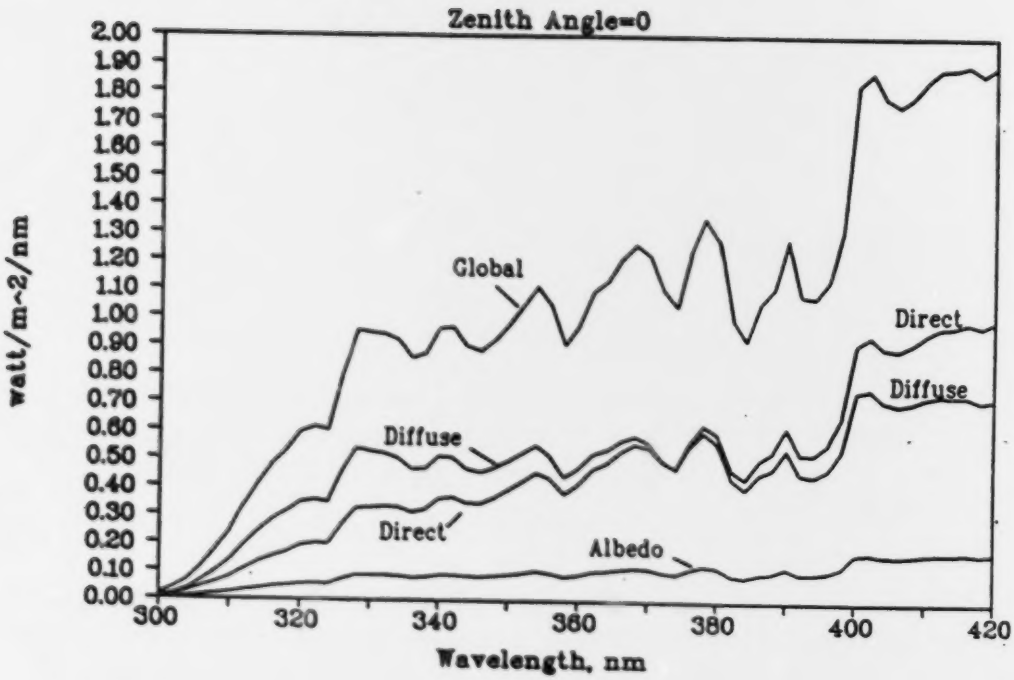

Figure 3. Example of Spectral Irradiance Components. Calculated from Schippnick and Green Fit to Dave Irradiance Model using World Radiation Center extraterrestial solar irradiance.

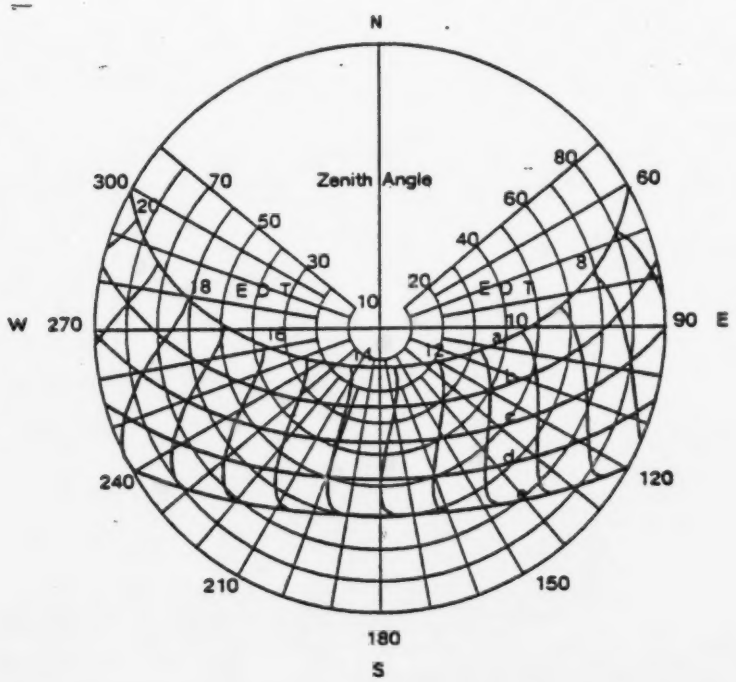

Figure 4. Sun's Position in the sky at a location in central North Carolina For Five Months: a) June 22; b) August 24; c) Sept. 23; d) October 24, e) Dec. 22. Numbers along top arc are Eastern Daylight Time.

Because of the sun's apparent motion through the sky, the path length traversed by photons reaching the surface varies as a function of time of day and location on the earth's surface. Longer atmospheric paths provide more opportunity for scattering and absorption. Thus, the relative contributions of diffuse and direct radiation to global radiation varies as a function of local solar coordinates (zenith angle). In addition, each "place" has a unique set of daily solar coordinates for each day of each year. Figure 4 illustrates the approximate solar coordinates for central NC for selected days in five months.

Radiation Models

Radiative transfer models have been developed to predict the global spectral irradiance using measured values of $\mathcal{H}_\lambda$ and descriptions of the atmospheric absorption and scattering processes. One such complex model developed by Dave[5] was used by Peterson[6] to predict the actinic irradiance at the earth's surface, and at several altitudes. This model assumed a cloudless, plane parallel, non-homogeneous atmosphere. The model atmosphere was divided into 40 layers, and each layer had unique properties: concentrations of air molecules, water vapor, carbon dioxide, and ozone; number density of aerosols; and temperature. A monochromatic unidirectional solar flux was incident at the top of the layers, and the surface at the bottom of the layers was an ideal diffuse reflector with a variable albedo. In each layer, the attenuated direct solar flux and upward and downward diffuse components were calculated.

The primary output of the Peterson model was presented as the actinic flux (units of photons-cm^{-2}-sec^{-1}) over 5-nm and 10-nm intervals from 295 nm to 700 nm at 10 zenith angles (χ =0°, 10°, 20°, ... 86°) for albedos of 0.0 and 0.05. In addition, the changes in flux with altitude and albedo of 0.10 were also described. The actinic flux was predicted to increase with distance above the surface. This is due not so much to increased absorption of the downward component as it is to a decrease in the upward component when approaching the ground. That is, when well above the surface there is a downward directed component, as well as a significant upward directed component (about 1/3 of total flux) caused by reflection from the air molecules and aerosols below. At or near the surface the downward component is about the same at higher up, but the upward component is much less (about 1/9 of the total flux) because the ground is not as reflective as several kilometers of air. Near the surface, then, the total spherical flux is lower than further away from the surface mostly because the upward component is lower near the surface. Later we will show albedos measured at different altitudes. The higher altitude albedos were much larger than the surface albedos as would be expected based on the above description.

Schippnick and Green[7] have fitted a series of analytical functions to all five of the Dave irradiance models and to Peterson's actinic flux model. These functions use as input: extraterrestrial flux, solar zenith angle, altitude (0 to 5 km), and surface albedo (0-0.3). They approximate, to a high accuracy, the original computer simulation outputs allowing for the simultaneous calculation of global irradiance on a horizontal surface (what meteorological instruments measure) and the actinic flux, or global spherical irradiance (what a molecule absorbs). This Schippnick and Green model is used throughout this chapter to produce the various irradiances

shown. An updating of the actinic flux calculation methods are needed, however, because the World Radiation Center values for $\mathcal{H}_\lambda$ are lower than the values used by Peterson and newer information is available on aerosol properties which will affect the calculated actinic fluxes. Because there is no need to compute and match global irradiance measurements in OZIPM model applications, the original Peterson fluxes, with their older assumptions of $\mathcal{H}_\lambda$ and other gas and aerosol distributions were used in Chapters 3 and 4 photolytic rate calculations so as to be consistent with other workers.

Albedo

In his 1976 calculations, Peterson assumed that 0.05 was the "best" albedo in the UV region. It is important to distinguish between the "regional" albedo, which will affect the area wide amount of light reflected upward to be scattered back downward, and the "local" albedo such as the surface under a spherical sensor. The present literature is not conclusive as to what are reasonable values for albedos in the UV region, and some satellite data suggests values as high as 0.15. Figure 5 illustrates the calculated actinic irradiance in the ultraviolet region (295–400 nm) at 0° zenith angle, at sea level for regional albedos of 0.05 and 0.15. These values probably represent the range of available photon flux for a primary photolysis reaction at the earth's surface in this wavelength region.

Kinetics Parameters

In effect, the absorption cross section is "how big an area" the molecule presents to the photon flux at each wavelength. At a given wavelength, a large cross section means that the molecule is more likely to absorb a photon, and therefore react.

Depending upon the energy in the absorbed photon, some molecules photodisassociate in more than one way. For example, formaldehyde (HCHO) photolysis can produce different products:

$$HCHO \xrightarrow{h\nu} H_2 + CO \qquad (2)$$

$$HCHO \xrightarrow{h\nu} H^{\cdot} + HCO^{\cdot} \qquad (3)$$

The quantum yield for a process is the ratio of the number of molecules that react by a given path to the number of molecules absorbing photons in the wavelength interval. For HCHO there would be two quantum yields, one for process (2) and one for process (3). Of course, the quantum yield for a given process or the combined quantum yields for all processes for a particular species cannot be greater than 1.0. A quantum yield of zero means that, although the molecule may absorb photons at

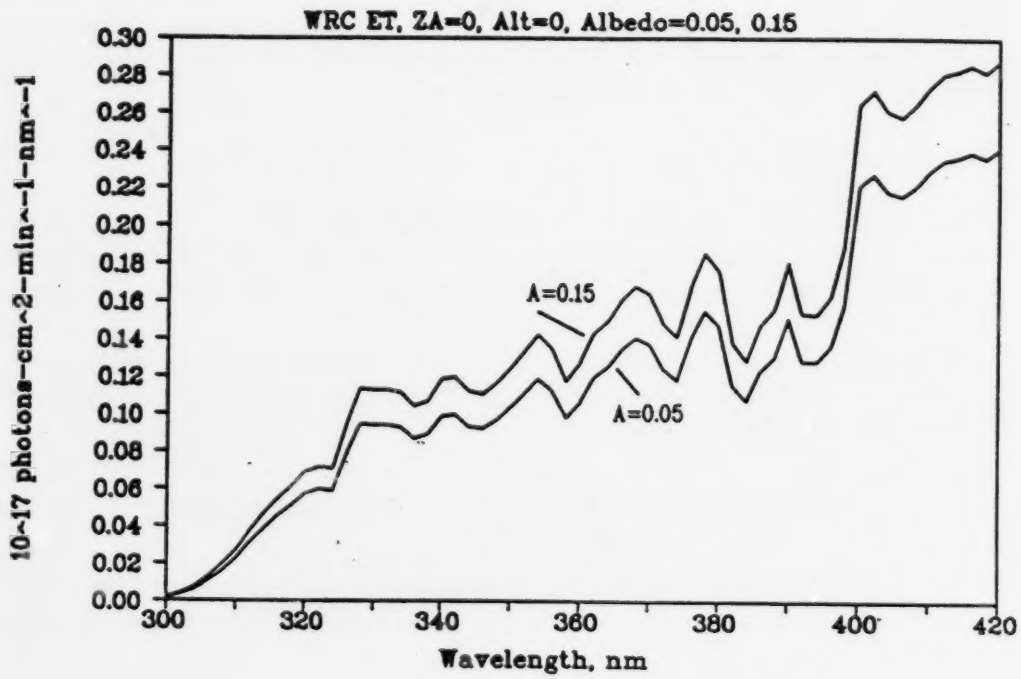

Figure 5. Theoretical Actinic or Spherical Irradiance at the Surface for Two Albedos.

the given wavelength, it does not undergo the given process. The quantum yield is dimensionless.

The absorption cross sections and quantum yields for a species must be measured in carefully controlled laboratory situations; they cannot be calculated theoretically. Newer measurements using better instruments have improved the accuracy and precision for these data and have resulted in a series of changes in calculated rates over the last 10 years. Evaluations of the experimental measurements have been published by various groups, such as NASA,[6] which recommend values for use primarily in stratospheric modeling. Sometimes, where there is some uncertainty, the absolute values of absorption cross sections have been estimated by "fits" to smog chamber experiments. That is, the measured values are used to define the relative spectral response, but the absolute magnitudes are scaled up or down as needed to fit model predictions to data.

Example Calculation

In this example, the actinic flux values are based on the WRC $\mathcal{A}_\lambda$ with a wavelength interval of 2 nm, centered at 300, 302, 304, ... Thus the σ_λ and Φ_λ values for each species must be averaged over the same 2 nm interval so that the area under the product curve will be correctly approximated. When this averaging is done, the integration operation in Equation 1 can be replaced by a summation over all the 2 nm intervals in which the product of the three components is not zero. For nitrogen dioxide (NO_2), for example:

$$J(\chi, y, A; NO_2) = \sum_{\lambda=300}^{420} \mathcal{A}_\lambda(\chi, y, A)\Delta\lambda\,\overline{\sigma}_\lambda(NO_2)\,\overline{\Phi}_\lambda(NO_2) \qquad (4)$$

where $\overline{\sigma}$ and $\overline{\Phi}$ represent 2-nm interval averaged values. Table 1 shows the calculation in tabular form for $\chi = 0°$, $y = 0$, $A = 0.05$. Figure 6 shows the same process in graphical form.

Some type of solar location program (astronomical almanac) is used to predict the zenith angle of the sun as a function of time for the particular location and day of the year. These predicted zenith angles are used to interpolate the species photolytic rates.

OZIPM Methods

Tables of Peterson's surface "actinic flux" as a function of wavelength and zenith angle for an albedo of 0.05 were incorporated as built-in data in the original OZIPP

Table 1. Calculation of Nitrogen Dioxide Photolysis Rate for Zenith Angle = 0°, altitude = 0 m, and albedo = 0.05.

λ	A_λ	$\overline{\sigma}_\lambda$	$\overline{\Phi}_\lambda$	$dJ/d\lambda^*$
300	0.0016	1.0685	1.0000	0.0171
302	0.0035	1.1700	0.9976	0.0409
304	0.0063	1.1700	0.9953	0.0734
306	0.0110	1.4150	0.9929	0.1546
308	0.0162	1.6600	0.9906	0.2664
310	0.0227	1.7100	0.9882	0.3836
312	0.0315	1.7600	0.9859	0.5466
314	0.0390	1.7600	0.9835	0.6751
316	0.0459	2.0050	0.9812	0.9030
318	0.0510	2.2500	0.9788	1.1232
320	0.0575	2.3950	0.9765	1.3447
322	0.0597	2.5400	0.9741	1.4771
324	0.0590	2.5400	0.9718	1.4563
⋮				
402	0.2277	6.7600	0.5650	8.6968
404	0.2182	6.7600	0.4050	5.9739
406	0.2160	6.5400	0.2875	4.0613
408	0.2213	6.3200	0.1900	2.6574
410	0.2293	6.0450	0.1375	1.9059
412	0.2351	5.7700	0.0914	1.2404
414	0.2366	5.7700	0.0743	1.0146
416	0.2394	5.5850	0.0572	0.7648
418	0.2363	5.4000	0.0401	0.5114
420	0.2415	5.4500	0.0230	0.3027
			$2\text{ nm} \times \sum_{300}^{420} dJ/d\lambda =$	0.4419 min^{-1}

* $dJ/d\lambda$ column has been multiplied by 1000

$$\frac{dJ}{d\lambda} = \left(\frac{10^{17}\,\text{photon}}{\text{cm}^2\text{-min-nm}}\right)\left(\frac{10^{-19}\,\text{cm}^2}{\text{molecule}}\right) = \text{min}^{-1}\text{-nm}^{-1}$$

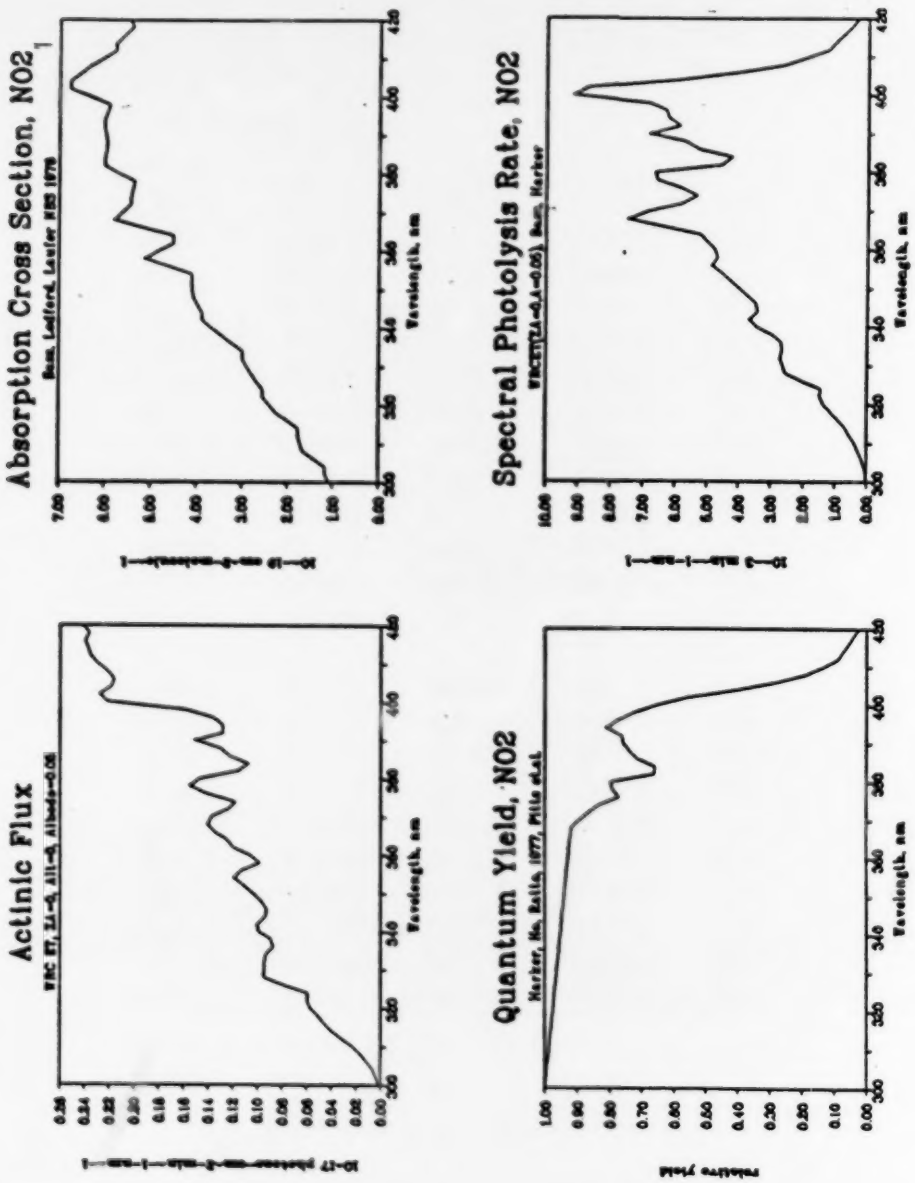

Figure 6. Calculation of Nitrogen Dioxide Photolysis Rate Using World Radiation Center 2-nm Extraterrestrial Spectrum, Albedo of 0.05, and Zenith Angle = 0°.

and OZIPM2 computer code. Similarly, species cross sections and quantum yields were also included as built-in data in OZIPP and OZIPM2. At the beginning of a simulation, these programs would calculate the species photolytic rates as a function of zenith angle and subsequently would interpolate these for the particular zenith angle needed at the time in the simulation. In the OZIPM3/4 code, the first step—calculation of species photolysis rate as a function of zenith angle—has been eliminated along with the built-in data for actinic flux and species cross sections and quantum yields. Instead, each species photolysis rate as a function of zenith angle is stored as built-in data. These were computed external to OZIPM3/4 using the method that was in OZIPM2, that is, using Peterson's actinic flux and up-to-date species cross sections and quantum yields. In OZIPM3/4, the user can also supply species photolysis rates as a function of zenith angle as part of his input, and thus override the built-in information.

Spectral Distribution of Rates

In the Carbon Bond Mechanisms, the most important photoacceptor species are: nitrogen dioxide (NO_2), formaldehyde (HCHO), ozone (O_3) photolyzing to atomic oxygen (O^{1D}), and acetaldehyde (RCHO). As described above, HCHO has two path ways: one to radicals (HCHO,R) and one to stable products (HCHO,S).

Using the actinic flux of Figure 5 (zenith angle of 0°) and currently recommended species cross sections and quantum yields, the *relative*, spectral photolysis rates (averaged over 10 nm intervals) of the four most important processes are shown in Figure 7 (the area under each species curve is scaled to unity). Acetaldehyde's rate is much less than HCHO, but its wavelength dependency is very similar to HCHO,R. In addition, the relative spectral response of the Eppley UV sensor is included. This sensor is commonly used in field measurements and is used by the University of North Carolina (UNC), SAI, and University of California at Riverside (UCR) modeling groups to derive or adjust theoretical photolysis rates for simulating experiments in the UNC and outdoor UCR chambers. The figure shows that the sensor only covers a part of the total actinic spectrum. The sensor's response is especially low at the short wavelengths where most of the photolysis of O_3 and HCHO,R occurs.

As shown in Figure 7, NO_2 has a broad photolysis spectrum, extending into the visible range (410 nm). O_3 has a very sharp photolysis spectrum, with more than half of the photolysis occurring in the interval 305–315 nm. This shorter end of the spectrum is more affected by path length (more scattering) and thus the photolysis rate of O_3 will decrease faster with increasing zenith angle than will that of NO_2.

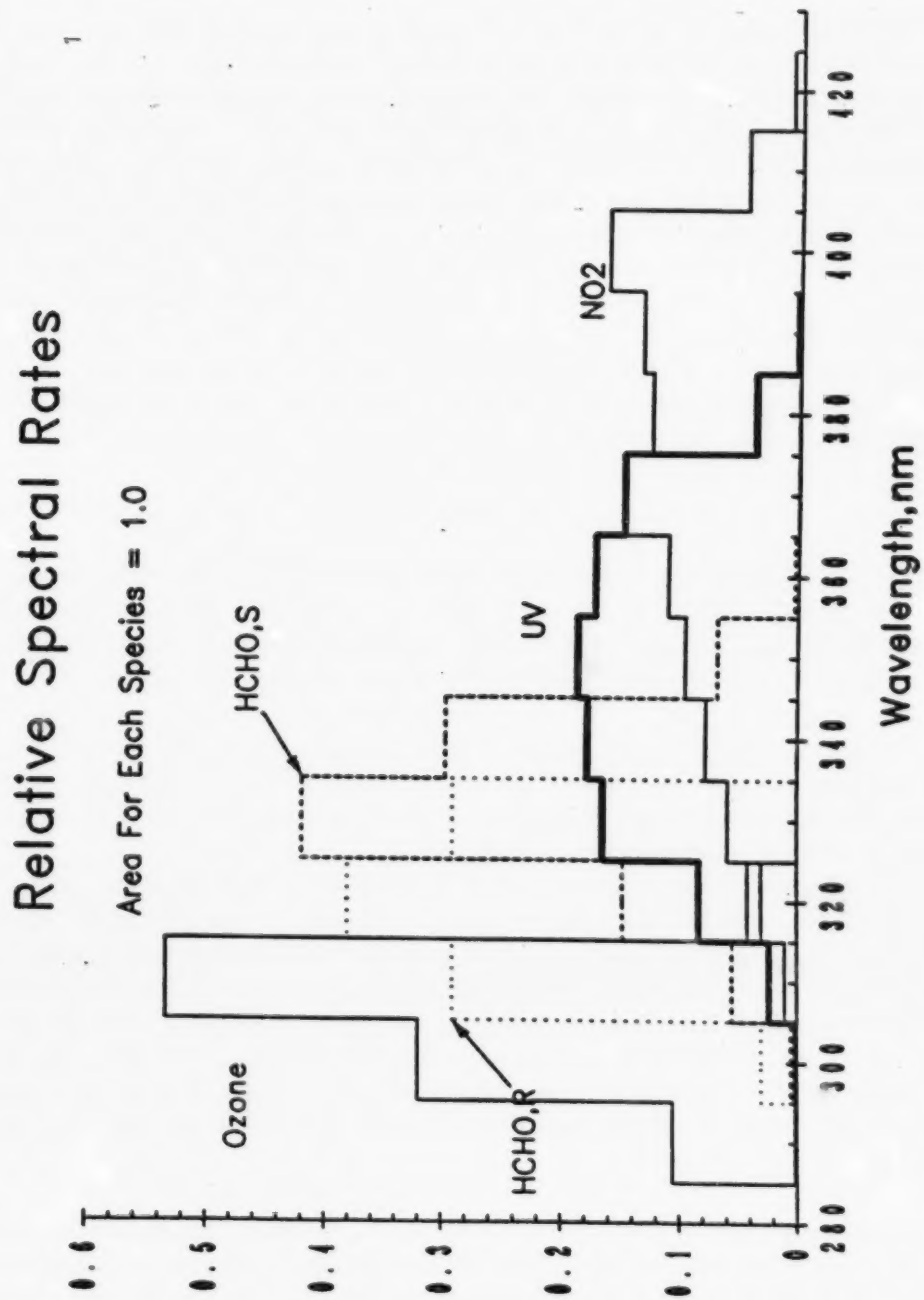

Figure 7. Relative Spectral Photolysis Rates.

HCHO shows a broader photolysis spectrum than O_3, and the rate is split between the two processes that produce stable and radical products. The radical process for HCHO is a very important source of radicals in all mechanisms.

2

Review of Calculated Rates

In this discussion, the photolytic rate data are presented as tables of rates vs. solar zenith angle. Because Whitten also used the ratio of each rate to the NO_2 rate, these ratio values are included (across the bottom of the tables) for comparison, but only at a zenith angle of zero. Table 2 explains the headings used in these tables. All of the rates used in all EPA models discussed in this report appear in Table 3, including the values recommended in this report. A few of these tables will appear again in later chapters as their method of calculation is explained.

Effects of Changes in Cross Section and Quantum Yield

The first set of theoretical rates used in EPA models were those of Schere and Demerjian, 1977[9] (See Table 3, heading Schere77). These rates were based upon the radiation model results of Peterson and the absorption cross sections and quantum yields as they were known at the time. The absorption cross section for NO_2 changed just as the report was being finished. An addendum was included giving the new rates calculated with the new absorption cross sections. The old rates compared to the new rates are shown to the right of the Schere77 table. This change subsequently caused problems in the photolytic rates incorporated into the OZIPP program code, and these will be discussed below.

The Demerjian, Schere, and Peterson 1980 report,[10] was a major revision of the 1977 work. In addition to using revised cross sections and quantum yield values, this work examined the effect of altitude and albedo on rates. The sea level rates are given in the Table 3, under the heading Demer80. The rates at various altitudes will be discussed later.

Carter's *et al.* final 1986 report[11] on the new surrogate species mechanism used reviewed information on cross sections and quantum yields as of February, 1986,

Table 2 Definitions of Headings used in Photolytic Rate Tables.

`Schere77`	The rates calculated by Schere and Demerjian in "Calculation of Selected Photolytic Rate Constants over a Diurnal Range," EPA-600/4-77-015, 1977.
`Demer80`	The rates calculated by Demerjian, Schere, and Peterson in "Theoretical Estimates of Actinic Flux and Photolytic Rate Constants for Atmospheric Species in the Lower Troposphere," *Adv. Environ. Sci. Technol.*, **29**, 1980.
`CB3,84`	The rates calculated by Killus and Whitten in "Technical Discussions Relating To the Use of Carbon Bond Mechanism in OZIPM/EKMA," EPA-450/4-84-009, 1984.
`Carter86,Surf`	The rates calculated by Carter, Lurmann, Atkinson, and Lloyd in "Development and Testing of a Surrogate Species Chemical Reaction Mechanism," Final Report, EPA Contract 68-02-4104, 1986.
`Whitten86,Surf`	The rates calculated by Whitten in "Using CBM-X in EKMA with Computer Code OZIPM-3"; these surface rates were not explicitly described in the report but were determined by back calculating from the altitude corrected values that were used in the final report.
`Whitten86,600m`	The rates calculated by Whitten in "Using CBM-X in EKMA with Computer Code OZIPM-3" after altitude corrections were applied to the surface rates.
`CB4,Surf,A=0.08`	The rates recommended in this document.
`CB4,640m,A=0.08`	The rates recommended in this document.

`ZA`	Zenith angle.
`J(NO2)`	Photolysis rate for NO_2 in units of min^{-1}.
`J(FR)`	Photolysis rate for HCHO to radicals in units of 1×10^{-3} min^{-1}.
`J(FS)`	Photolysis rate for HCHO to stable products in units of 1×10^{-3} min^{-1}.
`J(CR)`	Photolysis rate for CARB to radicals in units of 1×10^{-3} min^{-1}. See text for CARB composition.
`J(CS)`	Photolysis rate for CARB to stable products in units of 1×10^{-3} min^{-1}.
`J(O1D)`	Photolysis rate for O_3 to O^{1D} in units of 1×10^{-3} min^{-1}.
`J(CCHO)`	Photolysis rate for acetaldehyde to radicals in units of 1×10^{-3} min^{-1}.

Table 3. Theoretical Rates Used in EPA Models.

(all rates and ratios except NO_2 have been multiplied by 1000)
(all rates used $A = 0.05$ except those marked otherwise)

	Schere77				Old
ZA	J(NO2)	J(FR)	J(FS)	J(O1D)	J(NO2)
0	0.5129	2.14	5.60	4.210	0.5784
10	0.5087	2.11	5.53	4.110	0.5736
20	0.4963	2.01	5.33	3.730	0.5595
30	0.4741	1.85	4.98	3.160	0.5343
40	0.4395	1.61	4.45	2.420	0.4950
50	0.3880	1.30	3.73	1.610	0.4367
60	0.3168	0.92	2.84	0.840	0.3562
70	0.2058	0.49	1.62	0.280	0.2309
78	0.1014	0.20	0.72	0.060	0.1109
86	0.0221	0.04	0.15	0.007	0.0244
	1.00	4.17	10.92	8.21	

	Demer80			
ZA	J(NO2)	J(FR)	J(FS)	J(O1D)
0	0.5326	2.23	2.96	2.710
10	0.5282	2.20	2.92	2.630
20	0.5159	2.09	2.81	2.360
30	0.4922	1.90	2.61	1.960
40	0.4562	1.62	2.32	1.460
50	0.4026	1.27	1.92	0.930
60	0.3287	0.86	1.41	0.470
70	0.2132	0.43	0.80	0.150
78	0.1050	0.16	0.34	0.030
86	0.0229	0.03	0.07	0.003
	1.00	4.19	5.56	5.09

Table 3, cont. Theoretical Rates Used in EPA Models.

(all rates and ratios except NO_2 have been multiplied by 1000)

	Carter86,Surf				
ZA	J(NO2)	J(FR)	J(FS)	J(O1D)	J(CCHO)
0	0.4595	1.81	2.78	2.267	0.292
10	0.4559	1.79	2.75	2.197	0.286
20	0.4445	1.70	2.65	1.979	0.265
30	0.4245	1.54	2.47	1.634	0.230
40	0.3934	1.32	2.21	1.217	0.186
50	0.3472	1.04	1.84	0.775	0.133
60	0.2798	0.71	1.37	0.380	0.078
70	0.1840	0.36	0.79	0.119	0.032
78	0.0907	0.14	0.35	0.028	0.010
86	0.0194	0.02	0.07	0.003	0.002
	1.00	3.95	6.05	4.93	0.63

	Whitten86,Surf			
ZA	J(NO2)	J(FR)	J(FS)	J(O1D)
0	0.5129	1.39	1.93	2.390
10	0.5087	1.37	1.91	2.310
20	0.4973	1.30	1.84	2.060
30	0.4741	1.18	1.71	1.670
40	0.4395	1.00	1.52	1.220
50	0.3880	0.78	1.27	0.745
60	0.3168	0.52	0.95	0.352
70	0.2058	0.26	0.53	0.098
78	0.1014	0.10	0.23	0.021
86	0.0221	0.02	0.05	0.002
	1.00	2.71	3.78	4.66

Table 3, cont. Theoretical Rates Used in EPA Models.

(all rates and ratios except NO_2 have been multiplied by 1000)

	CB3,84			
ZA	J(NO2)	J(FR)	J(FS)	J(O1D)
0	0.5129	1.74	2.06	2.390
10	0.5087	1.71	2.05	2.310
20	0.4973	1.64	1.97	2.060
30	0.4741	1.49	1.83	1.670
40	0.4395	1.30	1.65	1.220
50	0.3880	1.05	1.38	0.745
60	0.3168	0.74	1.05	0.352
70	0.2058	0.40	0.60	0.098
80	0.1014	0.16	0.26	0.021
86	0.0221	0.03	0.06	0.002
	1.00	3.39	4.02	4.66

	Whitten86,600m			
ZA	J(NO2)	J(FR)	J(FS)	J(O1D)
0	0.6000	1.79	2.39	3.240
10	0.5952	1.79	2.39	3.150
20	0.5856	1.68	2.29	2.820
30	0.5642	1.54	2.15	2.310
40	0.5318	1.33	1.95	1.710
50	0.4851	1.07	1.68	1.080
60	0.4087	0.74	1.30	0.530
70	0.2882	0.40	0.79	0.160
80	0.1552	0.16	0.38	0.040
86	0.0348	0.03	0.08	0.005
	1.00	2.98	3.98	5.40

Table 3, cont. Theoretical Rates Used in EPA Models.

(all rates and ratios except NO_2 have been multiplied by 1000)

	CB4, Surf, A=0.08				
ZA	J(NO2)	J(FR)	J(FS)	J(O1D)	J(CCHO)
0	0.5358	1.89	2.98	2.310	0.301
10	0.5312	1.85	2.94	2.232	0.294
20	0.5166	1.76	2.83	2.003	0.272
30	0.4911	1.59	2.63	1.650	0.236
40	0.4524	1.36	2.34	1.216	0.189
50	0.3969	1.06	1.95	0.764	0.134
60	0.3184	0.71	1.44	0.371	0.079
70	0.2094	0.36	0.83	0.113	0.032
78	0.1025	0.14	0.37	0.024	0.010
86	0.0196	0.04	0.10	0.003	0.002
	1.00	3.53	5.56	4.31	0.56

	CB4, 640m, A=0.08				
ZA	J(NO2)	J(FR)	J(FS)	J(O1D)	J(CCHO)
0	0.5893	2.18	3.39	2.715	0.347
10	0.5851	2.14	3.35	2.620	0.338
20	0.5713	2.04	3.24	2.362	0.314
30	0.5470	1.86	3.03	1.962	0.275
40	0.5093	1.60	2.72	1.463	0.222
50	0.4537	1.27	2.30	0.944	0.161
60	0.3740	0.87	1.73	0.462	0.096
70	0.2578	0.45	1.03	0.140	0.041
78	0.1341	0.17	0.47	0.030	0.012
86	0.0242	0.04	0.13	0.003	0.002
	1.00	3.70	5.75	4.61	0.59

including corrections for errors that occurred in the printing of some previous reviews of photolysis rates (personal communication from Carter, 1986). Photolytic rates calculated from the cross sections and quantum yields used by Carter *et al.* and the Peterson 1976 actinic fluxes are shown in the Table 3, under the heading Carter86. These rates were calculated by his program which assumes that all input values were points connected by straight lines, even though HCHO data, for example, were given as 10-nm interval averages centered at the wavelength. The NO_2 cross sections and quantum yields used by Carter are the same as those recommended by Atkinson and Lloyd in their 1984 review.[12] The NO_2 absorption cross sections were the same as those used in the Schere77 addendum (Bass *et al.* data), and these are still the recommended values in the latest NASA review.[8] The quantum yields used in the 1977 work, the 1980 work, and in Carter's work were different, however.

The CB3.84 values were described in Killus and Whitten's 1984 technical discussion document[13] on the OZIPM2 program. The values in Table 3, however, were extracted from the computer code and the CARB rates have been converted back to HCHO rates. This rates will be described in detail in the next section.

The Whitten86.Surf values in Table 3 were calculated by us using information in the final report[1] "Using CBM-X in EKMA with Computer Code OZIPM-3" and in the computer code. These values do not actually appear in the final report, but are the basis of the altitude adjusted values that were recommended. The altitude adjusted rates are given in the table headed Whitten86.600m in Table 3. The latter two tables should be compared with the table headed CB3.84 in Table 3.

A recent (November 1986) intercomparison of photolytic rates was conducted by Jeffries (UNC) among Schere (EPA), Carter (UCR), Lurmann (ERT), Whitten and Gery (SAI) to establish a uniform treatment and to agree on sources of cross sections and quantum yields for use in model testing. NASA[8] was the source for NO_2, HCHO, and O_3. Carter *et al.*[11] was the source for CH_3CHO. These cross sections and quantum yields were integrated (depending upon whether the original values were point values or interval averages) and re-interpolated to 5-nm interval averaged values for use with Peterson's surface actinic flux data. The 5-nm interval averaged cross sections and quantum yields are given in Table 4.

The data in Table 4 were used with Peterson's surface flux, an albedo correction, and ratios of 640 meter photolysis rates to surface photolysis rates from the Demerjian *et al.* 1980 report to calculate the rates recommended in this report. The exact process will be described in Chapter 4. The resulting rates are given in Table 3 with the headings CB4.Surf.A=0.08 and CB4.640m.A=0.08.

Figure 8 compares four species rates from these studies. Figure 9 compares the quantum yields for NO_2 used in the Demer80 calculation and in the Carter86 calculation. The different Φ_λ assumptions were responsible for the differences in the NO_2 rates shown in Figure 8.

Values Calculated For Carbon Bond III in OZIPM2

In the previous "Technical Discussions Relating To the Use of Carbon Bond Mechanism in OZIPM/EKMA,"[13] Killus and Whitten describe the calculation of photolysis rates for CB3 in the OZIPM2 model. The method differed somewhat from the procedure described in the introduction above.

Because OZIPM2 still had the Dodge Mechanism as the built-in default mechanism, the built-in photolysis data had to be applicable to that mechanism. Thus the photolytic data stored in OZIPM2 were the Peterson 1976 actinic flux and the Schere and Demerjian 1977 cross sections and quantum yields. In effect the values shown in Table 3, heading Schere77 were the rate constants built into the program.

At the time Carbon Bond III was implemented in OZIPM2, significant changes had occurred in the cross sections and quantum yield values compared to the ones used in the Dodge mechanism, and thus the program calculated photolysis rates had to be corrected. In addition, the Demerjian, *et al.*, 1980 study had shown that photolysis rates should increase with altitude. Because the mixing height in OZIPM2 often extended to 1500 m in typical applications, Killus and Whitten also wanted to increase the calculated photolytic rates to account for this altitude effect.

Finally, in the CB3 mechanism, carbonyls are combined into a single species CARB. The characteristics of CARB were based on its approximating a mixture in photochemical equilibrium with a constant composition:

Species	Carbon Fraction
Formaldehyde	0.55
Higher Aldehydes	0.35
Glyoxal	0.05
Ketones	0.05

Thus, another correction factor had to be used to account for the CARB composition. In Table 12 of the 1984 technical discussion report, the ratio of CARB photolysis to HCHO photolysis was estimated to be 0.696 for radical product photolysis processes and 0.65 for stable product photolysis processes. Thus the "true" HCHO radical

Table 4. Absorption Cross Sections and Quantum Yields

(cross sections are 10^{-20} cm^2-$molecule^{-1}$, base e)

	NO_2		HCHO,R*		HCHO,S*		CH_3CHO		O^{1D}	
nm	σ	ϕ	σ	ϕ	σ	ϕ	σ	ϕ	σ	ϕ
295–300	10.7	0.982	2.62	0.78	2.62	0.22	4.24	0.453	55.81	0.900
300–305	14.1	0.978	2.62	0.78	2.62	0.22	3.73	0.370	28.84	0.898
305–310	17.1	0.974	2.45	0.77	2.45	0.23	3.07	0.280	14.98	0.753
310–315	20.1	0.970	2.45	0.77	2.45	0.23	2.41	0.193	7.56	0.311
315–320	24.0	0.966	1.85	0.62	1.85	0.38	1.85	0.113	3.87	0.043
320–325	26.7	0.962	1.85	0.62	1.85	0.38	1.37	0.053	2.02	0
325–330	28.9	0.958	1.76	0.31	1.76	0.69	0.91	0.015		
330–335	32.2	0.954	1.76	0.31	1.76	0.69	0.34	0		
335–340	36.7	0.950	1.18	0	1.18	0.69				
340–345	39.8	0.946	1.18	0	1.18	0.69				
345–350	40.9	0.942	0.42	0	0.42	0.40				
350–355	46.2	0.938	0.42	0	0.42	0.40				
355–360	48.2	0.934	0.06	0	0.06	0.12				
360–365	51.5	0.930	0.06	0	0.06	0.12				
365–370	56.0	0.926								
370–375	53.9	0.922								
375–380	56.7	0.845								
380–385	59.7	0.745								
385–390	59.7	0.793								
390–395	59.5	0.867								
395–400	63.3	0.795								
400–405	65.4	0.552								
405–410	60.5	0.241								
410–415	55.9	0.092								
415–420	54.5	0.045								
420–425	55.0	0.012								

All σ and ϕ values were averaged over 5-nm intervals except those marked with *, which were averaged over 10-nm intervals (*e.g.*, 295–305, 305–315), and therefore each of these values appears twice for the 5-nm averaged actinic flux data (*e.g.*, once for 295–300, once for 300–305).

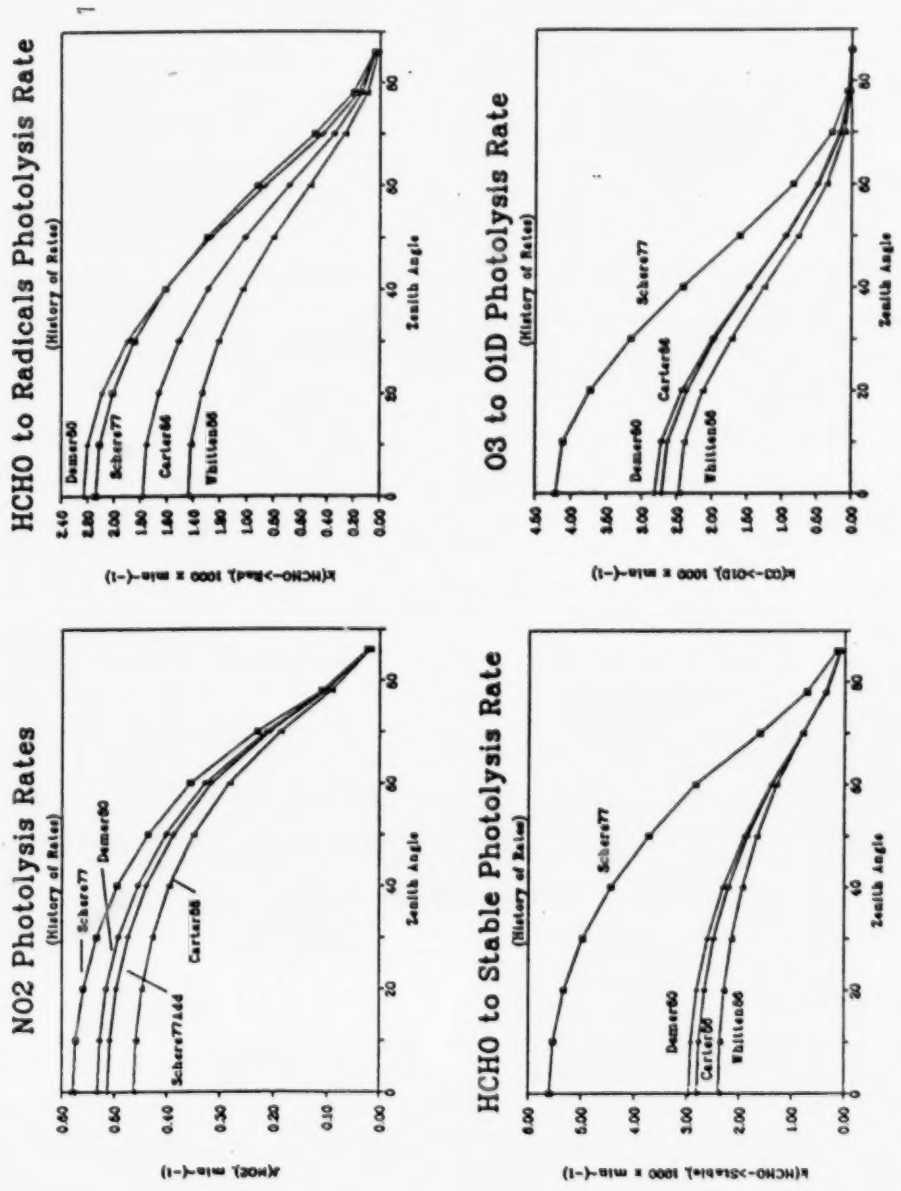

Figure 8. Photolysis Rates Calculated From Peterson 1976 Actinic Flux

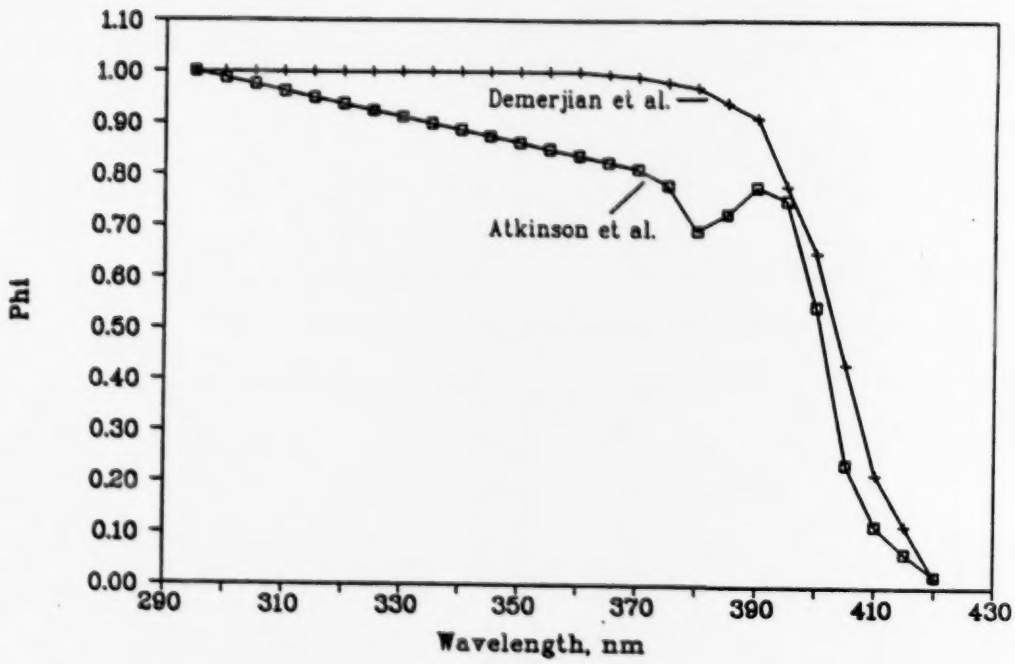

Figure 9. Quantum Yields For Nitrogen Dioxide Photolysis.

photolysis rate would be multiplied by 0.696 to account for the composition of CARB.

So many corrections increased the likelihood of errors, and some were made in the final specification of the photolysis rates for CB3 used in OZIPM2.

The table headed CB3.84 in Table 3 gives the photolysis rates used by CB3 in OZIPM2. These were computed by using built-in data in the OZIPM2 code. For discussion purposes, the CB3 CARB rate has been converted back into HCHO radical and stable rates in this table by "un-doing" the CARB composition correction described above. For example the CARB to radicals rate at $\chi = 0°$ was 1.21 min^{-1} in the OZIPM2 program. The rate given in the table headed CB3.84 in Table 3 is 1.74 = 1.21/0.696, which would be the true HCHO,R photolysis rate assumed by Killus and Whitten. Likewise, the HCHO,S rate in Table 3 was calculated as 2.06 = 1.34/0.65.

Nitrogen Dioxide Photolysis in CB3/OZIPM2

Killus and Whitten consulted the Demerjian *et al.*, 1980 report to determine what the $J(NO_2)$ values should be for CB3 when used in OZIPM2. The rates listed in the 1980 report at a zenith angle of zero were

y, meters	$J(0°, y, 0.05; NO_2)$
0	0.5328
150	0.5652
640	0.6216

In Table 9 of the Technical Discussion report,[13] Killus and Whitten indicated that OZIPM2 computed $J(\chi, 0, 0.05; NO_2)$ according to the older cross section data in the Schere and Demerjian 1977 report which would give a value at $\chi = 0°$ of 0.5784 min^{-1}. Thus Killus and Whitten assumed that, with no changes, OZIPM2 would calculate $J(NO_2)$ values that were comparable to those for an altitude somewhere inbetween 150 and 640 meters using the newer data (which would have been about a 9% increase compared to the ground value). Therefore, no changes were made to the 1977 NO_2 photolysis rates calculated by OZIPM2 for use with CB3.

Inspection of the OZIPM2 computer code, however, shows that Killus and Whitten were mistaken about the values built-in to OZIPM2; the values from the *addendum* for the Schere and Demerjian report were the ones actually used in OZIPM2. These gave a $J(NO_2)$ value at $\chi = 0°$ of 0.5129 min^{-1}, *less than the ground level rate in the Demerjian et al., 1980 data* and only 89% of the value that SAI thought they were using.

Carbonyl Photolysis in CB3/OZIPM2

Comparison of rates in Table 3 and Figure 8 shows that, compared to the rates stored in the OZIPM2 program, the HCHO rates had decreased significantly by the time Killus and Whitten were putting CB3 into OZIPM2. They showed, in Table 10 of their Technical Discussion,[13] that using what they thought was the Schere and Demerjian 1977 data stored in OZIPM2, gives the ratios

$$\frac{J(0°, 0, 0.05; \text{HCHO}, R)}{J(0°, 0, 0.05; \text{NO}_2)} = 3.70 \times 10^{-3}$$

$$\frac{J(0°, 0, 0.05; \text{HCHO}, S)}{J(0°, 0, 0.05; \text{NO}_2)} = 9.68 \times 10^{-3}$$

Based on their modeling of smog chamber experiments, however, Killus and Whitten had to use lower rates to obtain good fits, and thus they concluded that better ratios would be

$$\frac{J(0°, 0, 0.05; \text{HCHO}, R)}{J(0°, 0, 0.05; \text{NO}_2)} = 2.71 \times 10^{-3}$$

$$\frac{J(0°, 0, 0.05; \text{HCHO}, S)}{J(0°, 0, 0.05; \text{NO}_2)} = 3.76 \times 10^{-3}$$

Thus, Killus and Whitten stated that the built-in HCHO photolysis rates in OZIPM2 should be corrected by $2.71/3.7 = 0.73$ for radicals and by $3.76/9.68 = 0.37$ for stable products. Although the 0.37 "quantum yield update correction factor" appears in Table 12 of the Killus and Whitten report,[13] the 0.73 factor appears in the Table 12 as 0.78. The actual "quantum yield update correction factor" used, however, was 0.81 (shown by the final total correction factor being 0.564 which is 0.81×0.696, the CARB to HCHO correction factor from above). Killus and Whitten argue (on page 42 of reference 13) that the difference between the 0.73 and the 0.81 accounts for the increase in HCHO photolysis rate with height (which would have been about an 11% increase).

The wrong assumption about which set of NO_2 rates were built-in to OZIPM2, however, caused these ratios to be wrong. The actual Schere and Demerjian 1977 data stored in OZIPM2 had the following ratios:

$$\frac{J(0°, 0, 0.05; \text{HCHO}, R)}{J(0°, 0, 0.05; \text{NO}_2)} = 4.17 \times 10^{-3}$$

$$\frac{J(0°, 0, 0.05; \text{HCHO}, S)}{J(0°, 0, 0.05; \text{NO}_2)} = 10.92 \times 10^{-3}$$

and the correct "correction factors" would have been 2.71/4.17 = 0.65 for radicals and 3.76/10.92 = 0.35 for stable products. Even using 0.81 as the correction factor instead of the 0.65, however, did not compensate for the difference in the NO_2 photolysis rates, and thus the actual rates used were not at all what was intended.

Comparison of the HCHO photolysis rates plots in Figure 8 shows that, *in atmospheric applications*, CB3 in OZIPM2 had what are now known to be low values of HCHO photolysis rates, and therefore most likely would have a lower atmospheric reactivity than it should have. It would thus be quite sensitive to 'external' radical sources, such as NMOC aloft as has been determined in several SIP-like cases.[14] This large sensitivity is probably not correct, because it is most likely an artifact of the anomalously low HCHO photolysis rates.

A major reason for Killus and Whitten having chosen low ratios for $J(HCHO)/J(NO_2)$ was that these values produced the best fits to a large number of UNC outdoor smog chamber experiments. Recent measurements of the irradiance inside and outside the UNC chamber has shown, however, that the Teflon chamber walls are not 100% transparent in the 300–400 nm region. Further, the interaction between the film transmission and the reflective floor of the chamber results in the NO_2 photolysis rate being slightly higher inside the chamber than outside the chamber, while the HCHO photolysis is lower inside than outside. The best fits are produced by using the CB4.Surf.A=0.08 values for the atmospheric (outside chamber) and using a chamber light model that accounts for both the film transmission and the floor albedo. This model has been described by Jeffries and Sexton.[15] Thus, while the lower HCHO photolysis rates chosen by Killus and Whitten are appropriate when simulating the chamber, they are inappropriate when modeling the atmosphere.

Ozone Photolysis in CB3/OZIPM2

Killus and Whitten applied a large correction factor to the O_3 photolysis rate built-in to OZIPM2. Part of the correction was due to changes in the cross section data reported by Demerjian *et al.*, 1980, but a further correction was made to reduce the photolysis rate based on some atmospheric measurements. The final correction was 0.53 times the Schere and Demerjian 1977 rates. This resulted in rates that were slightly higher (6%) than the surface rates calculated by Carter *et al.*. in 1986.

How CB3/OZIPM2 Rates Influenced CB4/OZIPM3/4 Rates

The base set of values used to calculate the CB4 photolytic rates recommended by Whitten in his final report[1] are listed under the heading Whitten86.Surf in Table 3. By comparing these with the CB3.84 rates and with the values of $J(HCHO)/J(NO_2)$ (*e.g.*, 2.71 and 3.76) described by Killus and Whitten in their Technical Discussion report, you can see that the errors made in the earlier work were carried forward. Thus the values recommended by Whitten in his 1986 report depended upon the Schere77 NO_2 rates, upon the empirically determined value of HCHO-to-NO_2 photolysis rates for inside the UNC chamber, and upon the ratio-adjusted Schere77 ozone photolytic rates. Because the ultimate recommendations, the values listed under Whitten86.600m in Table 3, incorporated a *new* altitude correct not used in CB3/OZIPM2, the actual sources of the recommended rates were hard to determine. The final report recommendations were simply the values listed under Whitten86.Surf corrected to a higher altitude. So while the final recommended values were similar to the values recommended in this report, the technical support for the recommendations were lacking.

Affect of Altitude on Photolysis Rates

As indicated above, the Demerjian *et al.* 1980 study computed rates as a function of altitude and showed large increases (factors up to 1.5 times the surface rate). Because the mixing height often extends to 1500 meters in OZIPM3/4 applications, the photolytic rates should be increased above the surface values. We will assume that the rates at 640 meters can serve as approximate average rates for a 0–1500 meter mixing depth. Table 5 gives the NO_2 rates computed by Demerjian *et al.* 1980 for 0, 640, and 1380 meters. We will assume that the relative ratios of these values reflect the altitude effect and that these ratios can be used to adjust surface computed rates using somewhat different assumptions of σ_λ, and Φ_λ. Thus Table 5 includes, at the bottom, the ratio of the 640 m rate to the surface (0 m) rate when the ground albedo is 0.05. Whitten used these ratios and the values in Whitten86.Surf to compute Whitten86.600m, *e.g.*, $0.5129 \times 1.17 = 0.6001$. We will perform a similar adjustment for our recommended rates later in Chapter 4.

Table 5 Nitrogen Dioxide Photolysis Rate as a Function of Altitude.

	Demer80-Altitude		
ZA	J(NO2)0	J(NO2)640	J(NO2)1380
0	0.5326	0.6216	0.6834
10	0.5282	0.6180	0.6678
20	0.5159	0.6072	0.6576
30	0.4922	0.5868	0.6384
40	0.4562	0.5538	0.6072
50	0.4026	0.5028	0.5568
60	0.3287	0.4236	0.4770
70	0.2132	0.3000	0.3486
78	0.1050	0.1602	0.1962
86	0.0229	0.0312	0.0372
	1.00	1.17	1.28

	Ratio 640 to 0 m, A=0.05			
ZA	NO2	HCHOR	HCHOS	O1D
0	1.17	1.28	1.24	1.36
10	1.17	1.28	1.24	1.35
20	1.20	1.29	1.25	1.38
30	1.20	1.31	1.27	1.39
40	1.21	1.33	1.29	1.42
50	1.25	1.37	1.32	1.46
60	1.29	1.42	1.37	1.51
70	1.40	1.49	1.44	1.58
78	1.53	1.52	1.49	1.67
86	1.37	1.50	1.45	1.00

3

Atmospheric Rates

Measurements of Nitrogen Dioxide Photolysis Rates

A number of measurements of the atmospheric photolysis rate of NO_2 have been conducted.[16,17,18,19,20] Two sets of measurements, for example, are shown in Figure 10 from the Harvey, Steadman, Chameides work in 1977. The j_1 refers to the measured NO_2 photolysis rates using a quartz flow reactor, and the Eppley UV values were measured with the same type instrument as used at UNC. The points are the measured values, the line were computed by Harvey *et al.* using 1977 theory and are not relevant here. You should notice that *the maximum measured $j(NO_2)$ photolysis rates are greater than the theoretically calculated maximum NO_2 photolysis rate at a zenith angle of 0° given the presently accepted cross sections and quantum yields of Table 4 and the Peterson actinic flux at A = 0.05.* That is, using the "best" values of $\sigma_\lambda(NO_2)$ and $\Phi_\lambda(NO_2)$ and the Peterson actinic irradiances for "best case" albedo, the predicted maximum value is 0.503 min^{-1}, compared with a measured value of about 0.54–0.55 min^{-1}. Thus measurements are about 1.1 times larger than theory.

Parrish *et al.* conducted an NO_2 actinometry study in Colorado[19] in 1983. They could fit their clear sky values with an equation of the form

$$j(NO_2) = 0.7830\, e^{-0.360 \sec \chi} \quad min^{-1} \tag{5}$$

and all clear sky measurements fell within ±7% of this equation. This equation predicts a $\chi = 0°$ value of 0.5463 min^{-1}, in close agreement with that shown in Figure 10 for Michigan, but also larger than values predicted by present theory.

Comparison of Theory and Measurement for Irradiance

There are only three items that can be adjusted in the theory to improve its agreement with NO_2 actinometry measurements: actinic flux, absorption cross sections, and quantum yields.

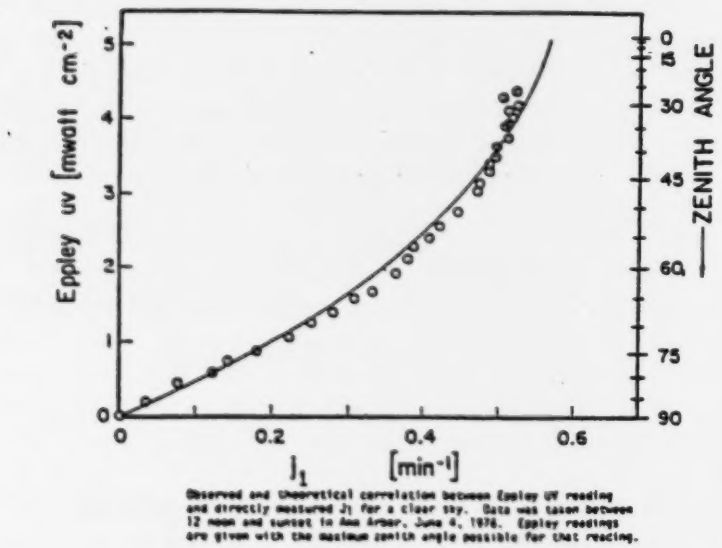

Observed and theoretical correlation between Eppley UV reading and directly measured j_1 for a clear sky. Data was taken between 12 noon and sunset in Ann Arbor, June 4, 1976. Eppley readings are given with the maximum zenith angle possible for that reading.

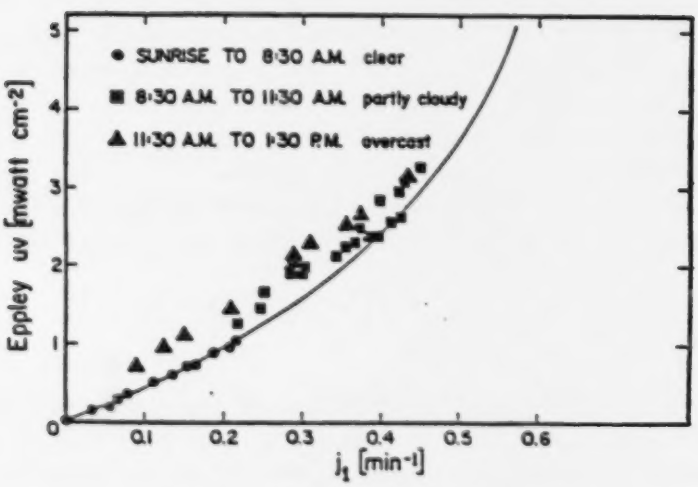

Observed correlation between Eppley and actinometer on May 29, 1976. The line is the theoretical prediction for a clear day

Figure 10. Examples of Measured Atmospheric Rates of Nitrogen Dioxide Photolysis.

The NO_2 cross section values in current use were obtained by Bass *et al.*,[21] with a resolution of 0.125 nm and an estimated absolute accuracy of ±10%. These values were generally confirmed in the range 375–420 nm by Harkner *et al.*,[22] who also established the quantum yield with a resolution of 1 nm in this same range. The low Φ_λ values reported by Harkner *et al.* for $\lambda > 375$ nm have been confirmed by Davenport.[23] Thus, while these factors may yet change with new measurements, there is no evidence for making *ad hoc* adjustments in these kinetic values, and we will continue to use the values as recommended by the NASA review.[8]

We have recently compared calculated global irradiance (300–420 nm region) with computerized spectroradiometer global irradiance measurements. The calculated values were produced by the Schippnick and Green[7] fits to the Dave spectral irradiance model and to the Peterson actinic flux model. We updated the extraterrestrial flux to the World Radiation Center 2-nm flux. We found excellent agreement over a zenith angle range of 14–80°. Examples of model predictions and measurements from shortly after sunrise to solar noon are shown in Figure 11.

As was shown in Figure 3, however, actinic flux, or spherical irradiance, has a significant upward component *that is not sensed by an upward looking, cosine response (flat) receiver such as the spectroradiometer or Eppley UV meter.* The downward scattering of this upward component has little effect on the flat, upward looking sensor, but as shown in Figure 12, an increase in surface albedo from 0.05 to 0.15 can have a large effect (22% increase) on global actinic irradiance while it only effects the global horizontal irradiance a small amount (< 2% increase). So the fact that the horizontal irradiance model can fit horizontal irradiance measurements still leaves the possibility that the regional albedo, or its impact on actinic flux may not be correctly represented in the Peterson "best estimate surface albedo" actinic flux data set.

UV Albedo

The present literature on ultraviolet albedo is not conclusive as to what are reasonable values for the "regional" albedo that should be used in the radiation transfer model calculations. Few spectrally resolved albedo values are available. Peterson used measured data from Coulson and Reynolds[24] to arrive at the spectral albedos shown in Table 6. Much of the literature only discusses the integral albedo, that is, the spectrally-weighted or "broadband" values. Using the solar spectrum in Figure 1, and the equation

$$A = \frac{\int_{\lambda_1}^{\lambda_2} A_\lambda \mathcal{A}_\lambda \, d\lambda}{\int_{\lambda_1}^{\lambda_2} \mathcal{A}_\lambda \, d\lambda}$$

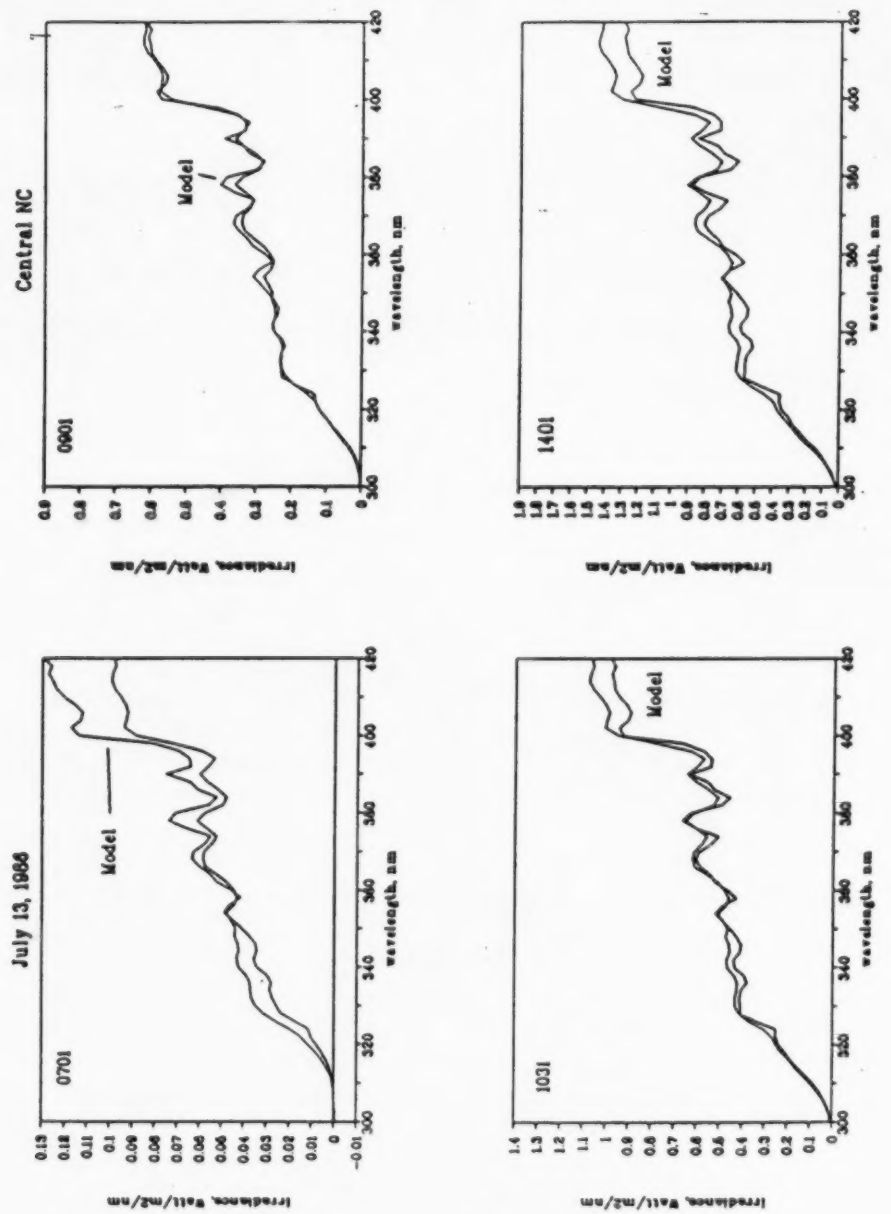

Figure 11. Comparison of Schippnick and Green Fit to Dave Radiation Model With LiCor 1800 Spectroradiometer Measurements, 2-nm intervals, 4-nm resolution.

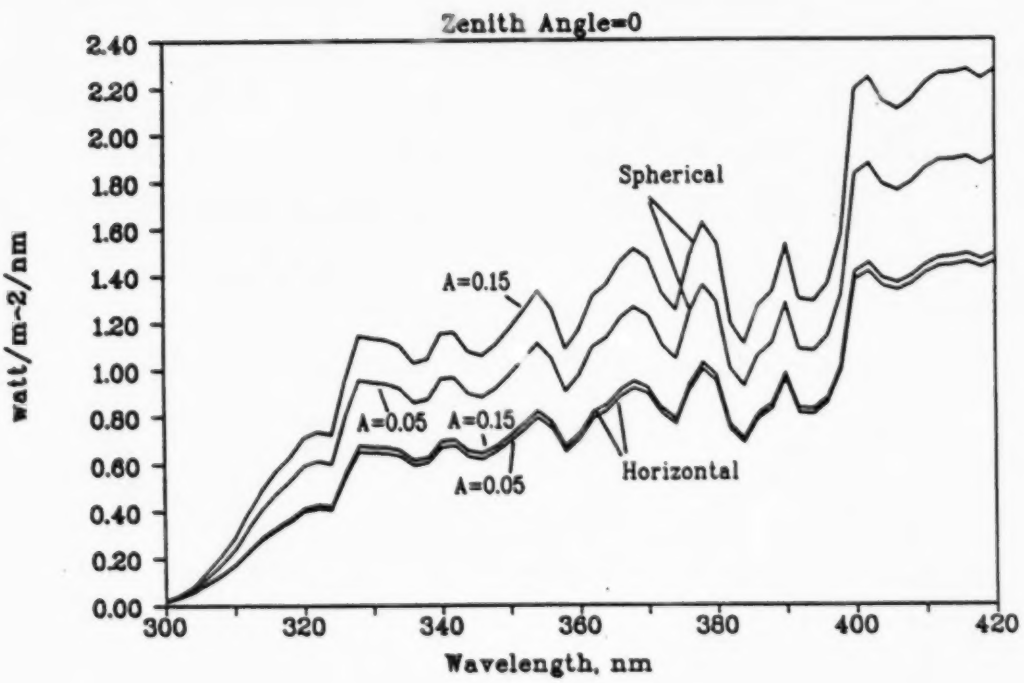

Figure 12. Comparison of Horizontal and Spherical Irradiance at Two Albedos.

we can calculate the integral albedo that matches Peterson's assumptions. By keeping Peterson's distribution assumptions as given in Table 6, but increasing the magnitudes uniformly, we can estimate both "broadband" or spectrally averaged albedo(A) and UV albedo (*e.g.*, A_{350}). For example,

increase	A	A_{350}
1.0	0.11	0.05
1.4	0.15	0.07
1.6	0.17	0.08
2.0	0.22	0.10

Dickerson *et al.*[18] reported albedos measured with the Eppley UV radiometer for various surfaces and from aircraft flights equipped with an upward and downward looking Eppley UV radiometer system. These are reported in Table 7. Doda and Green[25,26] also measured UV reflectances from airplanes. These researchers extrapolated their altitude data to the surface and estimated surface reflectivity. Some of their measurements are presented in Table 8. The Doda and Green values for pine forest are a factor of three lower than Dickerson's values for rain forest at the same altitude.

King and Herman[27] and King[28] calculated ground albedo from a statistical fit using empirically determined ratios of direct to diffuse light at a number of wavelengths. They determined a mean ground albedo of 0.279 at wavelengths of 521 and 670 nm for an area near the center of the city of Tucson AZ. This is significantly higher than the 0.10 value at 520 nm and the 0.15 value at 670 nm assumed in the Demerjian *et al.* 1980 study (see Table 6) suggesting that the values should be increased by nearly a factor of two.

Satellite data[29] indicate that the minimum integral albedo (200–4000 nm) over the U.S. is about 1.4 times higher than the 0.11 calculated from Demerjian *et al.* assumed values. The whole U.S. (except for the Western deserts which have minimum albedos of ≥ 0.20) has a minimum measured integral albedo of 0.15–0.20. Otterman and Fraser[30] used models of the scattering properties of the atmospheric aerosols and LANDSAT data for the southwest U.S. to calculate surface albedos of 0.264 in the region 500–600 nm with little sensitivity to the aerosol model assumed. This value is consistent with the values found by King, and reported by the NIMBUS 3 data[29] again suggesting that larger albedo values should be used in the photolytic rate calculations.

Using data from another satellite, the Atmosphere Explorer-E, Frederick and Abrams[31] also used a numerical model of radiative transfer, including multiple

Table 6. Albedo Values Assumed by Peterson.

λ	albedo
290–400	0.05
400–450	0.06
450–500	0.08
500–550	0.10
550–600	0.11
600–640	0.12
640–660	0.13
660–700	0.15

Table 7, a. Surface Albedo Values Measured by Dickerson *et al.*, using Eppley UV Radiometer.

surface	albedo
grass	0.01
black cloth	0.02
white plywood	0.07
road surface	0.07–0.09
cement	0.17

Table 7, b. Near Surface Albedo Values Measured by Dickerson *et al.* Using Modified Eppley UV Radiometer.

surface	altitude, km.	albedo
rain forest	0.05–0.30	0.06–0.18
high plains	0.3	0.12
	2.9	0.33

Table 8. UV Albedo Values Measured by Doda and Green.

surface	altitude, km.	albedo
pine forest	0.0–0.33	0.02–0.04
desert sand, w. Texas	0.0–0.33	0.05–0.07
gypsum sand, White Sands NM	0.0–0.33	0.16–0.19 (300 nm) 0.53–0.60 (400 nm)

scattering and surface reflection to calculate the distribution of albedo at two wavelengths, 331.2 and 339.8 nm. There were 7421 measurements; 69% produced albedo values less than 0.30 and higher values were interpreted to include reflection from clouds. Eleven percent of the albedo values were between 0.0 and 0.10, 29% were between 0.10 and 0.20, and 20% were between 0.20 and 0.30. As expected, there was no systematic variation of albedo with zenith angle.

Based on such recent evidence, other newer radiation models have used regional UV albedos of ≈ 0.15 (see for example Logan *et al.*[32]).

We will therefore multiply the values in Table 6 by 1.6 to obtain integral or "broadband" albedo of 0.17 and a UV albedo of 0.08. The value 0.08 will be used to adjust the actinic flux before photolytic rate calculations are performed in the rest of this report.

Adjustment of Calculated Actinic Flux for Albedo

Information is supplied in the Demerjian *et al.* 1980 study to estimate the effect of albedo changes up to 0.20. Demerjian *et al.* give a table of increases in actinic flux as a function of wavelength and zenith angle as albedo was increased from 0 to 0.10. They state that the changes were approximately linear with albedo. We have used this table to produce an albedo enhancement factor as a function of λ and χ. These factors are used to adjust the spectral actinic irradiance when computing rates.

If we apply a "regional" albedo correction to the Peterson actinic flux (that is, increase the albedo from 0.05 to 0.08), then surface NO_2 photolysis rates computed from σ_λ and Φ_λ in Table 4 are in much better agreement with Parrish *et al.* atmospheric measurements. Computed values are given in Table 9 and are shown in Figure 13. The values in Table 9 that are under the heading 'Fit to Observations' are predicted from Equation 5. The bottom line in Figure 13 shows (and the first column of Table 9 gives) the values predicted from theory using the Peterson actinic

fluxes and current cross sections and quantum yields. The second column (and the next higher line in Figure 13) is the result of assuming a "regional albedo" of 0.08 rather than 0.05 in the standard flux calculations. The third column is the result of applying the "site specific" corrections calculated by Parrish for his particular location (*e.g.*, elevation, aerosols, and total column O_3). The last column shows that the fitted observations and the theory agree to within about 2% for small zenith angles and within about 5% for large zenith angle where the site corrections are quite large.

Table 9. Comparison of Higher Albedo Calculated Photolysis Rates with Atmospheric Measurements.

	----Effect of Albedo on J(NO2)---				
ZA	A=0.05	A=0.15	SiteAdj	FitObs	Obs/Theory
0	0.5031	0.5358	0.5498	0.5463	0.99
10	0.4991	0.5312	0.5461	0.5433	0.99
20	0.4866	0.5166	0.5342	0.5338	1.00
30	0.4643	0.4911	0.5127	0.5167	1.01
40	0.4300	0.4524	0.4802	0.4894	1.02
50	0.3794	0.3969	0.4326	0.4472	1.03
60	0.3062	0.3184	0.3629	0.3811	1.05
70	0.2023	0.2094	0.2584	0.2733	1.06
78	0.0990	0.1025	0.1383	0.1386	1.00
86	0.0188	0.0196	0.0240	0.0045	

	----Adjustment Factors---		
ZA	Albedo	Site	Total
0	1.06	1.03	1.09
10	1.06	1.03	1.09
20	1.06	1.03	1.10
30	1.06	1.04	1.10
40	1.05	1.06	1.12
50	1.05	1.09	1.14
60	1.04	1.14	1.19
70	1.03	1.23	1.28
78	1.04	1.35	1.40
86	1.04	1.23	1.28

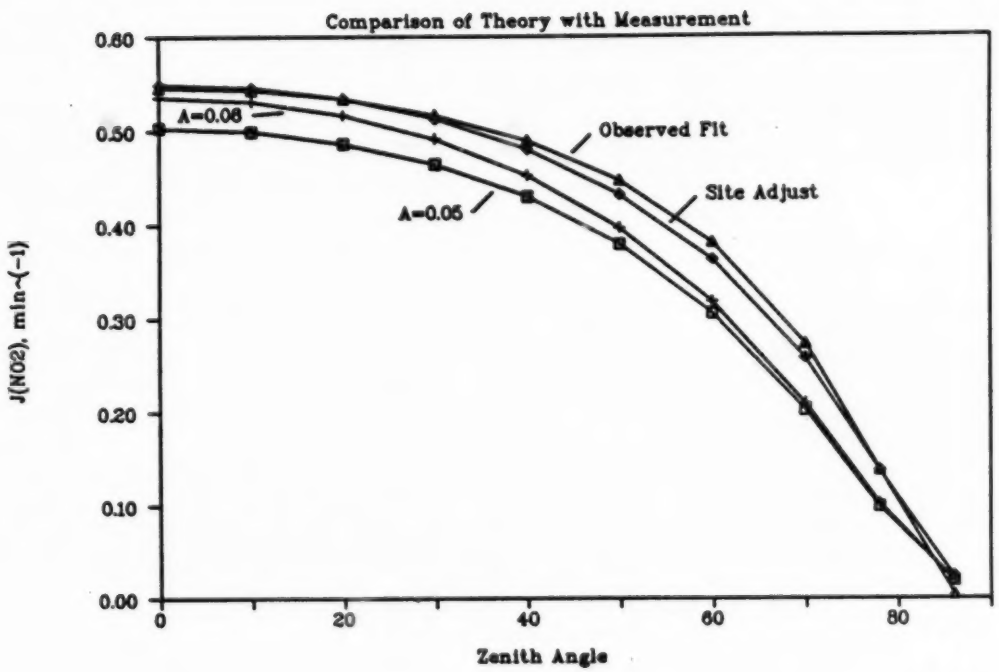

Figure 13. Comparisons of Adjusted Theory with Parrish *et al.* Measurements of Atmospheric NO_2 Photolysis Rates.[19]

4

Recommended Rates

In this chapter, the actinic flux, kinetics parameters, and altitude effects from Chapter 2 will be combined with the re-estimated best albedo value of 0.08 from Chapter 3 to estimate atmospheric rates at the surface and at 640 meters for use in OZIPM3/4 model program.

Rates for Carbon Bond IV in OZIPM3/4

Surface Rates

To compute surface rates, the actinic flux of Peterson, the albedo effect adjustment, and the cross sections and quantum yields given in Table 4 were used.

The resulting rates, which would be the values to use for CB4 in a ground level application, are shown in Table 10.

Mixed Layer Rates

As described near the end of Chapter 2, there is a strong effect of altitude on photolytic rates. This is because, as stated in Chapter 1, the air below a given altitude well above the ground has a greater reflectivity upward than the absorbing, low albedo ground. Therefore, the spherical flux at an altitude is higher than at the surface. Table 5 gave the ratio of photolysis rate at 640 m to that at 0 m for the "best albedo" assumptions of Demerjian *et al.* (0.05). If the albedo assumption of 0.05 is too low, then the ratios in Table 5 are too high because the surface values are too low. Thus the ratios in Table 5 are not appropriate to adjust the rates of Table 10.

As an approximation to the correct ratios for an albedo of 0.08, we will use the ratio of photolysis rates at 640 m to those at 150 m for an albedo of 0.05. That is,

we assume that

$$\frac{J(0°, 640, 0.05; \mathsf{S})}{J(0°, 150, 0.05; \mathsf{S})} \approx \frac{J(0°, 640, 0.08; \mathsf{S})}{J(0°, 0, 0.08; \mathsf{S})}$$

since at the higher albedo, there will be less difference between the higher altitude rates and the surface rates because the surface is more reflective. These ratios are shown in Table 11.

Applying the ratios of Table 11 to the surface values of Table 10, gives the recommended values for the mixed layer. These are shown in Table 12.

Recommended CB4 Photolytic Rates

The values in Table 12 are the photolytic rates that should be used in OZIPM3/4 with the Carbon Bond Four Mechanism when performing control strategy calculations.

Rates for Carbon Bond III in OZIPM3

Because of previous use of CB3 in making SIP calculations and because there were a number of errors made in calculating the photolytic rates in OZIPM2, we have made new recommendations for photolytic rates for use with CB3 in OZIPM3/4.

The calculation of these new CB3 rates follows the same procedure as that for CB4 except that the carbonyl weighting factor for radical processes and for stable process (see discussion in Chapter 2) has been recalculated and applied to the HCHO photolysis rates to produce the CARB photolysis rates. The original weighting factor for production of radicals (w_r) was

$$w_r = (0.55 + 0.005 + 0.0175)J(\mathsf{HCHO}, R) + 0.35(J(\mathsf{CH_3CHO})/J(\mathsf{HCHO}))$$

where the numerical coefficients reflect the CARB composition as described in Chapter 2. The coefficient of the last term, $J(\mathsf{CH_3CHO})/J(\mathsf{HCHO})$, changed from 0.35 to 0.16 for the new photolytic rates, thus lowering w_r to 0.602 compared to its old value of 0.695. The factor relating HCHO,S rates to CARB,S rates remains the same as before, 0.65.

The recommended rates for CB3 in OZIPM3/4 are given in Table 13 and Table 14.

Table 10. Recommended CB4 Surface Photolytic Rates.

(all rates and ratios except NO_2 have been multiplied by 1000)

	CB4,Surf,A=0.08				
ZA	J(NO2)	J(FR)	J(FS)	J(03)	J(CCHO)
0	0.5358	1.891	2.980	2.310	0.301
10	0.5312	1.859	2.943	2.232	0.294
20	0.5166	1.759	2.828	2.003	0.272
30	0.4911	1.593	2.631	1.650	0.236
40	0.4524	1.359	2.341	1.216	0.189
50	0.3969	1.062	1.947	0.764	0.134
60	0.3184	0.714	1.436	0.371	0.079
70	0.2094	0.360	0.830	0.113	0.032
78	0.1025	0.138	0.367	0.024	0.010
86	0.0196	0.036	0.103	0.003	0.002
	1.00	3.53	5.56	4.31	0.56

Table 11. Altitude Adjustments Corrected For Albedo.

	Ratio 640 to 150m, to approx A=0.08				
ZA	NO2	HCHOR	HCHOS	O1D	CCHO
0	1.10	1.15	1.14	1.17	1.15
10	1.10	1.15	1.14	1.17	1.15
20	1.11	1.16	1.14	1.18	1.16
30	1.11	1.17	1.15	1.19	1.17
40	1.13	1.18	1.16	1.20	1.17
50	1.14	1.20	1.18	1.24	1.20
60	1.17	1.22	1.21	1.25	1.22
70	1.23	1.24	1.25	1.24	1.26
78	1.31	1.24	1.27	1.25	1.26
86	1.24	1.20	1.23	1.00	1.17

Table 12 Recommended CB4 Mixed Layer Photolytic Rates.

(all rates except NO_2 have been multiplied by 1000)

	CB4,640m,A=0.08				
ZA	J(NO2)	J(FR)	J(FS)	J(03)	J(CCHO)
0	0.5893	2.179	3.391	2.715	0.347
10	0.5851	2.141	3.353	2.620	0.338
20	0.5713	2.036	3.237	2.362	0.314
30	0.5470	1.858	3.032	1.962	0.275
40	0.5093	1.599	2.724	1.463	0.222
50	0.4537	1.272	2.304	0.944	0.161
60	0.3740	0.873	1.732	0.462	0.096
70	0.2578	0.448	1.034	0.140	0.041
78	0.1341	0.172	0.466	0.030	0.012
86	0.0242	0.043	0.127	0.003	0.002
	1.00	3.70	5.75	4.61	0.59

Example Predictions Using New Rates

Simulation Conditions

To illustrate the effect of the new recommendations, some example simulations will be compared. Example 1 (CB4) and Example 2 (CB3), which were used in the OZIPM3 guidance document[1], were used as sources of conditions. The only difference between Example 1 and Example 2 was the change in mechanisms. Table 15 gives the simulation conditions. In all examples, the Characteristic Curve for Mixing Height was used. All simulations began at 0800 LDT and ran for 10 hours.

In the control cases, the initial HC was reduced by various amounts and no reduction occurred for NO_X.

Table 13. Recommended CB3 Surface Photolytic Rates.

(all rates except NO_2 have been multiplied by 1000)

	CB3,Surf,A=0.08			
ZA	J(NO2)	J(CR)	J(CS)	J(O3)
0	0.5358	1.139	1.937	2.310
10	0.5312	1.119	1.913	2.232
20	0.5166	1.061	1.838	2.003
30	0.4911	0.964	1.710	1.650
40	0.4524	0.827	1.522	1.216
50	0.3969	0.652	1.265	0.764
60	0.3184	0.447	0.933	0.371
70	0.2094	0.237	0.539	0.113
78	0.1025	0.104	0.239	0.024
86	0.0196	0.040	0.067	0.003
	1.00	2.13	3.62	4.31

Table 14. Recommended CB3 Mixed Layer Photolytic Rates.

(all rates except NO_2 have been multiplied by 1000)

	CB3,640m,A=0.08			
ZA	J(NO2)	J(CR)	J(CS)	J(O3)
0	0.5893	1.312	2.204	2.715
10	0.5851	1.289	2.180	2.620
20	0.5713	1.228	2.104	2.362
30	0.5470	1.124	1.971	1.962
40	0.5093	0.972	1.770	1.463
50	0.4537	0.781	1.498	0.944
60	0.3740	0.547	1.126	0.462
70	0.2578	0.295	0.672	0.140
78	0.1341	0.129	0.303	0.030
86	0.0242	0.048	0.083	0.003
	1.00	2.23	3.74	4.61

Table 15, a. Initial Conditions.

Item	Value	Units
Latitude	39.93	degrees
Longitude	75.10	degrees
Date	6/24/80	mm/dd/yy
Initial Mixing Ht.	250	meter
Final Mixing Ht.	1235	meter
Initial NMOC	1.100	ppmC
Initial NO_x	0.120	ppm
Surface NMOC	0.038	ppmC
Surface O_3	0.010	ppm
Aloft NMOC	0.040	ppmC
Aloft O_3	0.070	ppm
Temperature	303	K
Water Vapor	25000	ppm

Table 15, b. NMOC Fractions.

Source	PAR	ETH	OLE	TOL	XYL	RCHO	HCHO	NR
Emissions	0.51	0.04	0.03	0.12	0.10	0.03	0.02	0.16
Surface	0.53	0.05	0.03	0.07	0.06	0.16	0.10	0.00
Aloft	0.61	0.06	0.03	0.08	0.07	0.09	0.06	0.00

Table 15, c. Emissions Fractions.

Hour	1	2	3	4	5	6	7	8
NMOC	0.17	0.17	0.17	0.10	0.02	0.02	0.02	0.02
NO_x	0.35	0.35	0.35	0.19	0.03	0.03	0.03	0.07

Simulation Results

Figure 14 shows the NO, NO_2, and O_3 profiles for CB4 using the surface photolytic and 640 m photolytic rates from Tables 10 and 12 for the Example 1 case. The higher photolytic rates (mixed layer rates) resulted in about a 5% increase in predicted maximum O_3 for these conditions.

Figure 15 shows the NO, NO_2, and O_3 profiles for CB3 using the 640 m photolytic rates from Table 14 and the older 1984 photolytic rates from Table 3 for the Example 2 case. The higher photolytic rates (new rates) also resulted in a 5% increase in predicted maximum O_3 in this NO_X-limited situation. That the increase was not greater was caused by the fact that the much larger increase in CARB,S rates offset the increase in CARB,R rates and *less* CARB photolyzed to radicals in the simulation using the higher 640 m rates than did in the simulation using the 1984 rates. That is, the total CARB consumption by photolysis to stable products was 181% of the amount consumed with the 1984 rates, while the consumption by photolysis to radical products was 97% of the amount consumed by this process with the 1984 rates. Therefore, most of the increase using the new rates was due to the increased NO_2 photolytic rates as opposed to the higher CARB rates.

Figure 16 shows the NO, NO_2, and O_3 profiles for both CB3 and CB4 using the mixed layer photolytic rates. CB3 was initially more reactive than CB4 when using the same basic photolytic data. This was in part because of the constant composition CARB in CB3. Figure 17 shows the CARB profile from CB3 and the "calculated CARB" profile from CB4 (*i.e.*, HCHO+ 2 RCHO). CB3 maintained a high level of CARB in the middle of the simulation compared to CB4. This higher CARB level occured at the maximum photolysis rate and produced many more radicals in CB3 than in CB4, thus increasing its overall reactivity. The larger amount of radicals also resulted in a more rapid removal of the NO_X causing the O_3 profile to show a sharp decrease in rate at about 400 minutes. CB4 clearly has a more realistic treatment of the carbonyl chemistry than CB3.

Figure 18 shows the NO, NO_2, and O_3 profiles for CB4 using the mixed layer photolytic rates for: a) the Example 1 case, and b) the same conditions with a 40% HC reduction. The 40% HC reduction (*i.e.*, 1.10 to 0.66 ppmC) resulted in a 32% O_3 reduction (*i.e.*, 0.260 to 0.178 ppm).

Figure 19 shows the NO, NO_2, and O_3 profiles for CB3 using the new mixed layer photolytic rates for a) the Example 1 case, and b) the same conditions with a 40% HC reduction. The 40% HC reduction (*i.e.*, 1.10 to 0.66 ppmC) resulted in a 25% O_3 reduction, that is, less reduction than occurred with CB4. A partial explanation for

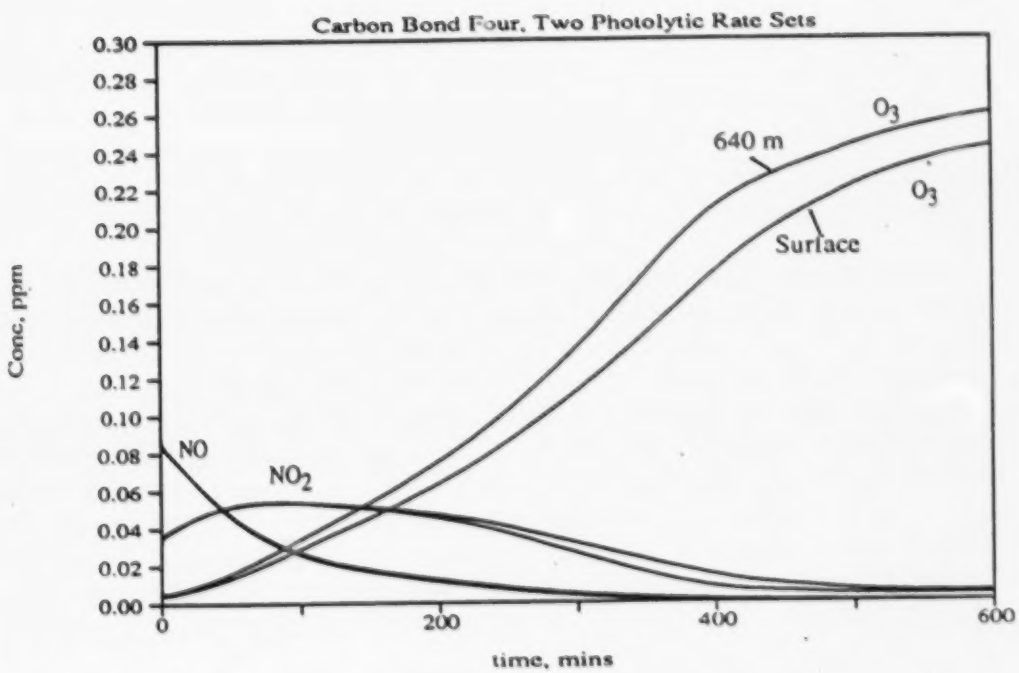

Figure 14. Example Simulation Using CB4: Comparison of Surface and Mixed Layer Photolytic Rates. (Example 1 from Guidelines for OZIPM3[1]).

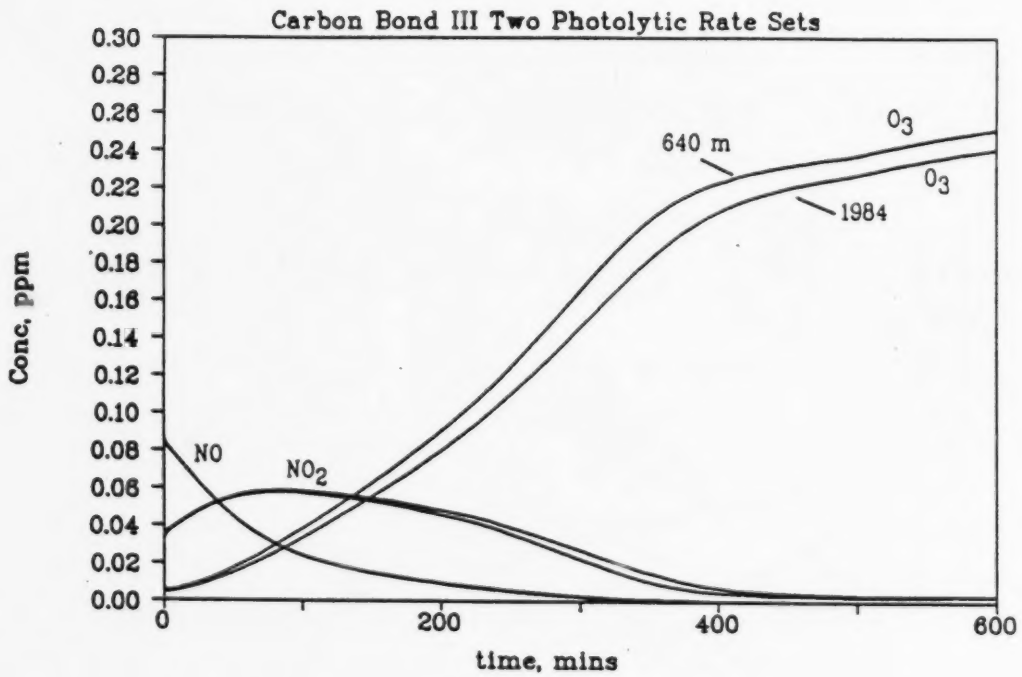

Figure 15. Example Simulation Using CB3: Comparison of Mixed Layer and 1984 Photolytic Rates. (Example 2 from Guidelines for OZIPM3[1]).

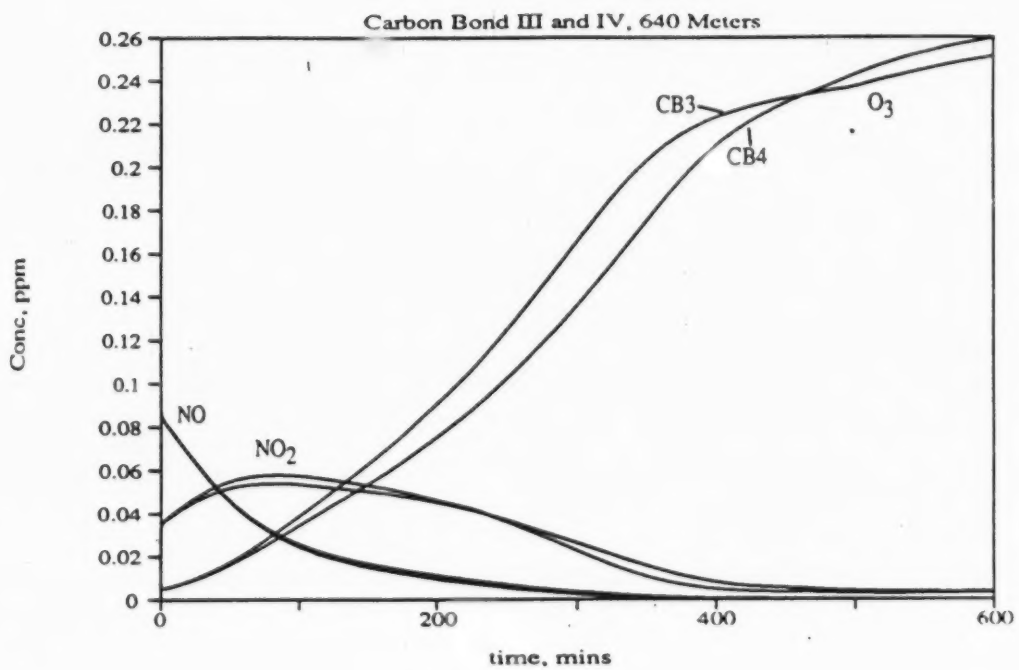

Figure 16. Comparison of CB3 and CB4 Using Mixed Layer Photolytic Rates.

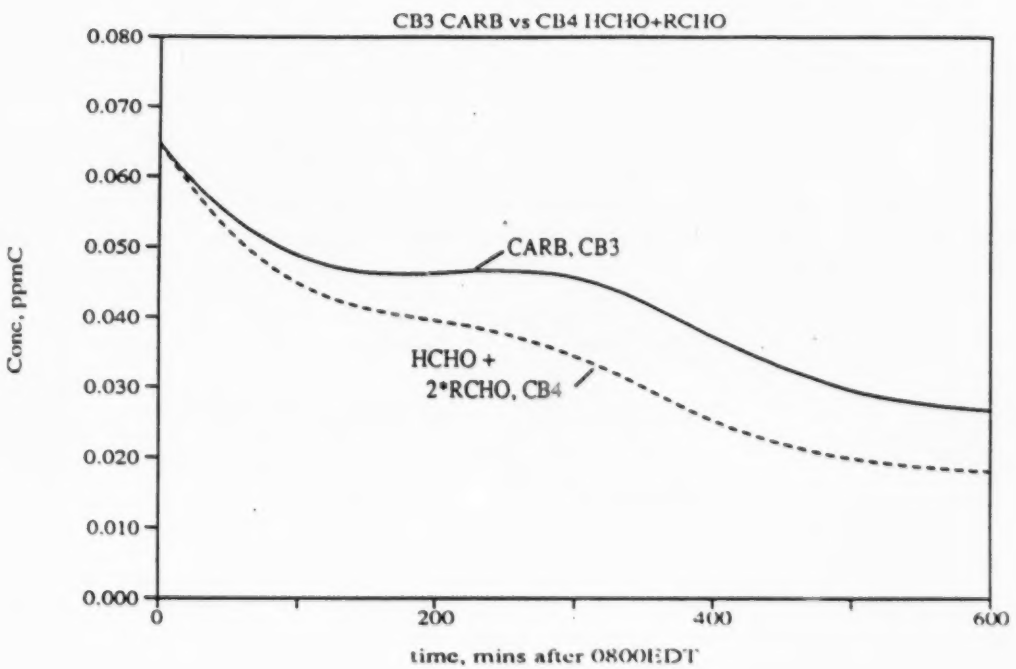

Figure 17. Comparison of CARB (CB3) and HCHO+RCHO (CB4) Using Mixed Layer Photolytic Rates.

the difference between the two mechanisms can be obtained from Figure 20. This figure shows the O_3–HC relationship for CB4, CB3 with older 1984 rates, and CB3 with the new mixed layer rates. All three profiles show a limiting of O_3 production with increasing HC, however, the CB4 profile shows a slightly "steeper" dependence of O_3 on HC. That is, CB4 made slightly more O_3 at higher HC and less O_3 at lower HC than did CB3. In these simulations, it is the relative difference in the CARB vs. HCHO profiles during the middle of the simulations that is the primary cause of the differences between CB3 and CB4 in this case.

Figure 20 also shows a typical control calculation. The base case O_3 is assumed to be 0.18 ppm. Each mechanism predicts a different HC level would be needed to produce this amount of O_3: 0.667 ppmC for CB4; 0.648 ppmC for CB3, 1984 rates; and 0.591 ppmC for CB3, new rates. The slopes of the three curves are similar between the 0.12 and 0.18 ppm O_3 lines; that is $\Delta O_3/\Delta HC$ values are: 0.335 ppm/ppmC for CB4; 0.320 ppm/ppmC for CB3, 1984; and 0.357 ppm/ppmC for CB3, new rates. Since the absolute reactivity of the three mechanisms is very close at the 0.18 ppm O_3 level, very similar control requirements are predicted for the different mechanisms:

$$27\% = 100\left(\frac{0.179}{0.668}\right) \quad \text{for CB4}$$

$$29\% = 100\left(\frac{0.187}{0.649}\right) \quad \text{for CB3,84}$$

$$28\% = 100\left(\frac{0.168}{0.591}\right) \quad \text{for CB3,new}$$

Although the three mechanisms gave similar results in this example, the improved treatment of carbonyl chemistry in the Carbon Bond Four mechanism makes it a superior mechanism compared to Carbon Bond Three and its predictions should more accurately reflect the effects of emissions and photolytic rate changes than those of Carbon Bond Three.

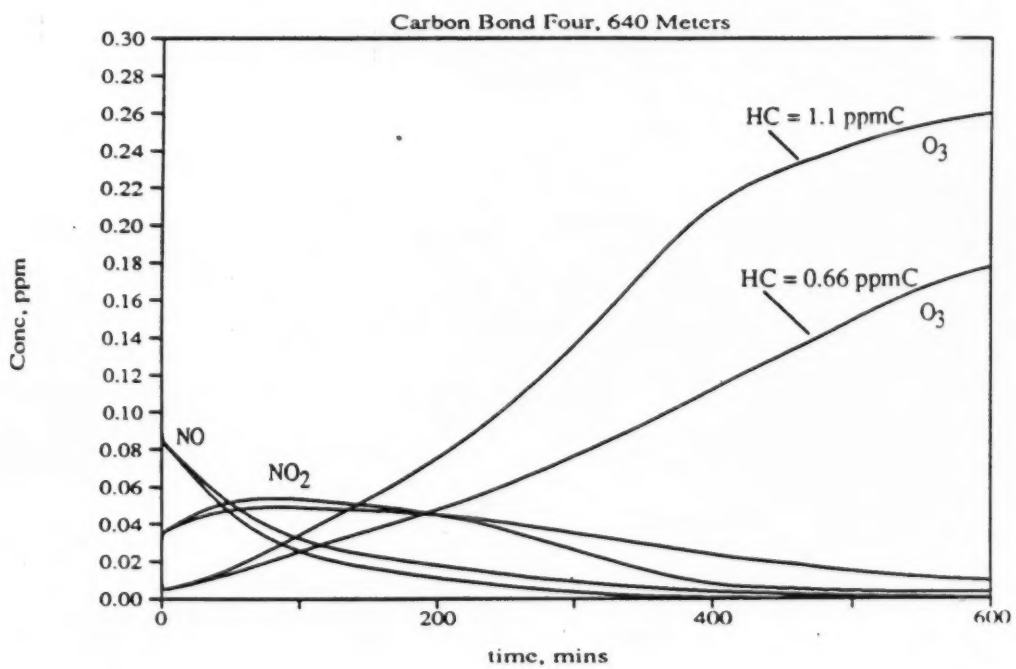

Figure 18. Example Simulation Using CB4: 40% HC Control Using Mixed Layer Photolytic Rates.

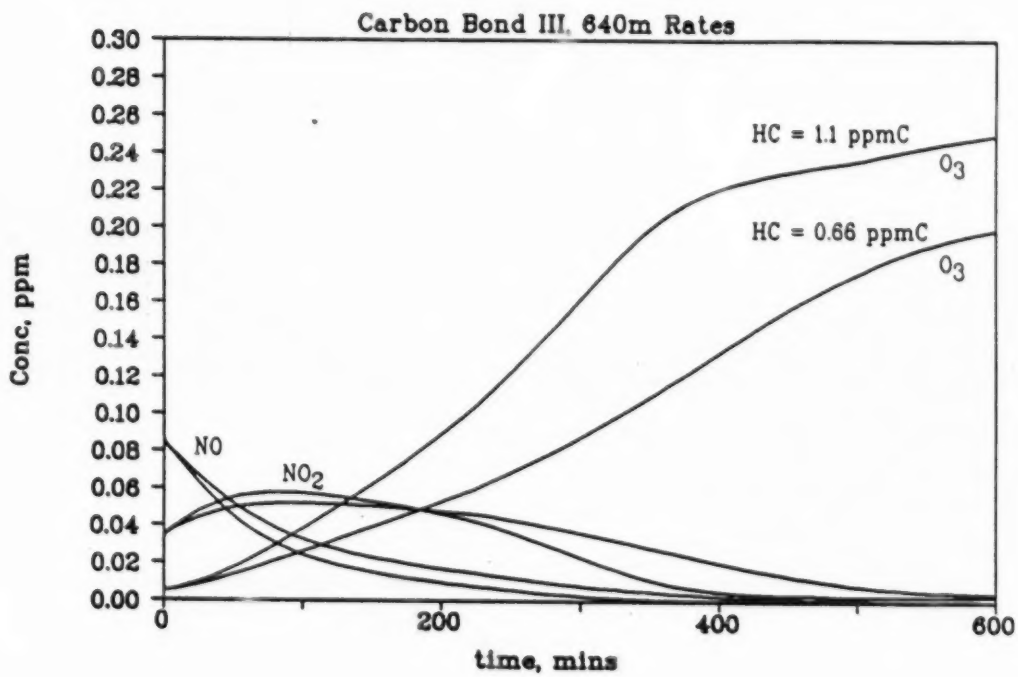

Figure 19. Example Simulation Using CB3: 40% HC Control Using 1984 Photolytic Rates.

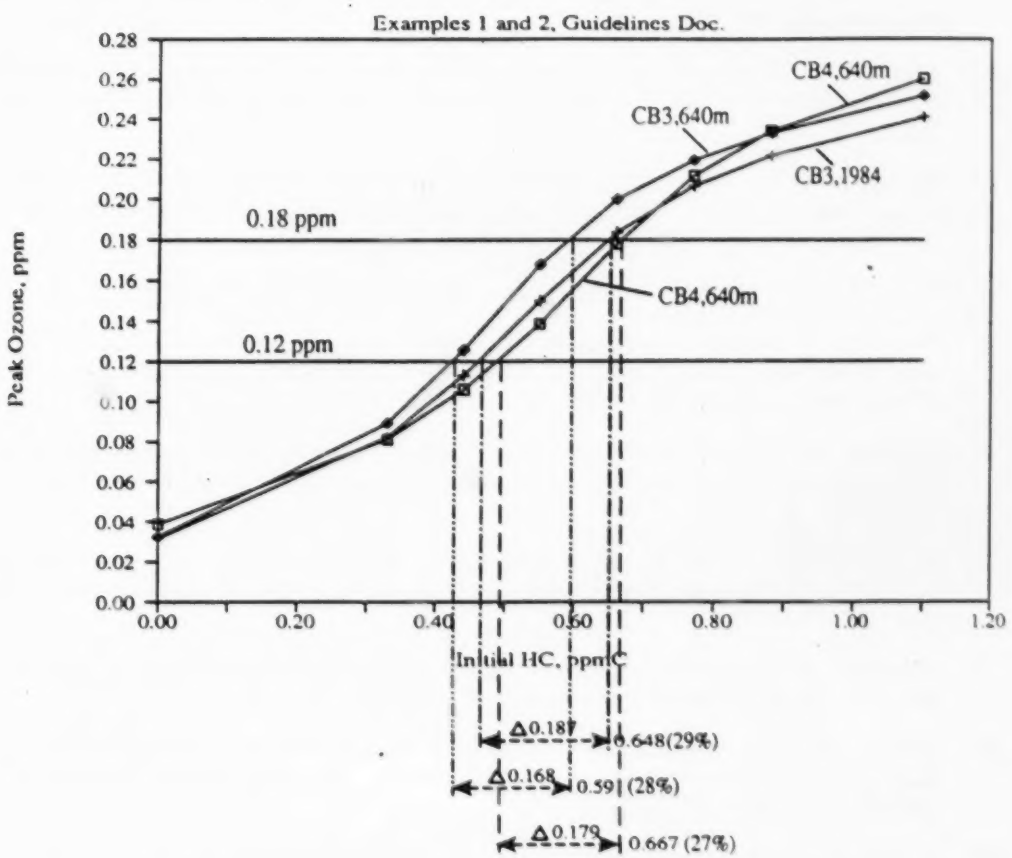

Figure 20. Comparison of Ozone-Hydrocarbon Relationships for CB3 and CB4.

References

1 H. Hogo, G.Z. Whitten,"Guidelines for using OZIPM3 with CBM-X or Optional Mechanisms," EPA/600/3-86/004, U.S. Environmental Protection Agency, Research Triangle Park, North Carolina, Jan 1986.

2 Whitten, G.Z., H. Hogo, "User's Manual for Kinetics Model and Ozone Isopleth Plotting Package," EPA-600/8-78-014a, U.S. Environmental Protection Agency, Research Triangle Park, NC, 1978.

3 Gipson, G.L. "User's Manual for OZIPM-2: Ozone Isopleth Plotting With Optional Mechanisms/Version 2," Office of Air Quality Planning and Standards, U.S. Environmental Protection Agency, Research Triangle Park, NC, 1984

4 Iqbal, M., "An Introduction to Solar Radiation," Academic Press, NY, 1983.

5 Dave, J.V.,"Development of Programs for Computing Characteristics of Ultraviolet Radiation," Final Report, NAS5-21680, NASA Report CR-139134, National Aeronautics and Space Administration, Goddard Space Flt. Ctr., Greenbelt, MD, 1971.

6 Peterson, J.T.,"Calculated Actinic Fluxes for Air Pollution Photochemistry Applications," EPA-600/4-76-002, U.S. Environmental Protection Agency, Research Triangle Park, NC, 1976.

7 Schippnick, P.F., A.E.S. Green, "Analytical Characterization of Spectral Actinic Flux and Spectral Irradiance in the Middle Ultraviolet," *Photochemistry and Photobiology*, **35**, pp 89–101, 1982.

8 "Chemical Kinetics and Photochemical Data for Use in Stratospheric Modeling," Evaluation #7, Jet Propulsion Laboratory Publication 85-37, 1985.

9 Schere, K.L. and K.L. Demerjian,"Calculation of Selected Photolytic Rate Constants over a Diurnal Range," EPA-600/4-77-015, U.S. Environmental Protection Agency, Research Triangle Park, NC, 1977.

10 Demerjian, K.L., K.L. Schere, and J.T. Peterson, "Theoretical Estimates of Actinic Flux and Photolytic Rate Constants for Atmospheric Species in the Lower Troposphere," *Adv. Environ. Sci. Technol.*, **29**, 1980.

11 Carter, William P.L., F.W. Lurmann, R. Atkinson, and A. Lloyd, "Development and Testing of a Surrogate Species Chemical Reaction Mechanism," Final Report, EPA Contract 68-02-4104, U.S. Environmental Protection Agency, Research Triangle Park, North Carolina, 1986

12 Atkinson, R. and Allen C. Lloyd, "Evaluation of Kinetic and Mechanistic Data for Modeling Photochemical Smog," *J. Chem. Ref. Data.* **13**, No. 2, p315–444, 1984.

13 Killus, J. and G.Z. Whitten, "Technical Discussions Relating To the Use of Carbon Bond

Mechanism in OZIPM/EKMA," EPA-450/4-84-009, U.S. Environmental Protection Agency, Research Triangle Park, NC, 1984.

14 Jeffries, H.E., K.G. Sexton, "Sensitivity of Carbon Bond Mechanism to NMOC aloft." Progress Report, Sensitivity of EKMA-type Control Estimates to Model Inputs, EPA Co-operative agreement CR812315, 1986

15 Jeffries, H.E. and K.G. Sexton, "UNC Chamber Photolytic Rate Calculation Procedure," Technical Guidance Report, Department of Environmental Science, UNC, Chapel Hill, NC, 1986.

16 Zafonte, L., P.L. Rieger, J.R. Holmes, "Nitrogen Dioxide Photolysis in the Los Angeles Atmosphere," *Envir. Sci. Techno.* **11** 5, pp 483–487, 1977.

17 Harvey R.B., D.H. Stedman, W. Chameides, "Determination of the Absolute Rate of Solar Photolysis of NO_2," *J.A.P.C.A.* **27**, 7 pp 663–665, 1977

18 Dickerson R.R., D.H. Steadman, A.C. Delany, "Direct Measurements of Ozone and Nitrogen Dioxide Photolysis Rates in the Troposphere," *J. Geo. Res.* **87**, pp 4933–4966, 1982.

19 Parrish, D.D., P.C. Murphy, D.L. Albritton, F.C. Fehsenfeld, "The Measurement of the Photodissociation Rate of NO_2 in the Atmosphere," *Atmos. Environ.* **17** pp 1365–1378, 1983.

20 Madronich S., D.R. Hastie, B.A. Ridley, H.I. Schiff, "Measurements of the Photodissociation Coefficient of NO_2 in the Atmosphere: I. Method and Surface Measurements," *Journal Atm. Chem.* **1** pp 3–25, 1983

21 Bass, A.M, A.E. Ledford, A.H. Laufer, "Extinction Coefficients of NO_2 and N_2O_4" *J. Res. NBS*, **80A**, No. 2, pp 143–166, 1976.

22 Harkner, A.B., W. Ho, J.J. Ratto, "Photodissociation Quantum Yield of NO_2 in the Region 375 to 420 nm," Chem. Phy. Lettr. **50**, No. 3, pp 394–397, 1977.

23 Davenport, J.E., "Determination of NO_2 Photolysis Parameters of Stratospheric Modeling," Report No. FAA-EQ-78-14, 1978.

24 Coulson, K.L. and D.W. Reynolds, *J. Appl. Meteorol.*,**10**, pp 1285, 1971.

25 Doda, D.D., A.E.S. Green, "Surface Reflectance Measurements in the UV from an Airborn Platform, Part 1," *Applied Optics* **19** pp 2140– 2145, 1980.

26 Doda, D.D., A.E.S. Green, "Surface Reflectance Measurements in the UV from an Airborn Platform, Part 2," *Applied Optics* **20** pp 636–642, 1981.

27 King, M.D., B.M. Herman, "Determination of the Ground Albedo and the Index of Absorption of Atmospheric Particulates by Remote Sensing. Part I: Theory.," *J. Atmos. Sciences* **36** pp 163–173, 1979.

28 King, M.D., "Determination of the Ground Albedo and the Index of Absorption of Atmospheric Particulates by Remote Sensing. Part II: Application," *J. Atmos. Sciences* **36** pp

1072–1083, 1979.

29 Raschke, E., T.H. Vander Harr, W.R. Bandeen, M. Pasternak, "The Annual Radiation Balance of the Earth-Atmosphere System During 1969–70 from Nimbus 3 Measurements," *J. Atmos. Sciences* **30**, pp 341–364, 1973.

30 Otterman, J., R.S. Fraser, "Earth-atmosphere System and Surface Reflectivities in Arid Regions from LANDSAT Data," *Remote Sens. Environ.* **5**, pp 247–266, 1976.

31 Frederick, J.E., R.B. Abrams, "The Surface Albedo of the Earth in the Near Ultraviolet (330–340 nm)," *Remote Sens. Environ.* **11**, pp 337–347, 1981.

32 Logan, J.A, M.J. Prather, S.C. Wofsy, M.B. McElory, "Tropospheric Chemistry: A Global Perspective," *J. Geo. Res.* **86** pp 7210–7254, 1981.

33 Jeffries, H.E., K.G. Sexton, C.N. Salmi, "The Effect of Chemistry and Meteorology on Ozone Control Calculations Using Simple Trajectory Models and the EKMA Procedure," EPA-450/4-81-034, U.S. Environmental Protection Agency, Research Triangle Park, NC, 1981.